LIMNOLOGY
AND
OCEANOGRAPHY

November 2000
Volume 45
Number 7

Limnol. Oceanogr., 45(7), 2000, 1449–1466

Organic matter in Bolivian tributaries of the Amazon River: A comparison to the lower mainstream

John I. Hedges,[1] *Emilio Mayorga, Elizabeth Tsamakis, Michael E. McClain, Anthony Aufdenkampe, Paul Quay, and Jeffrey E. Richey*
School of Oceanography, Box 357940, University of Washington, Seattle, Washington 98195-7940

Ron Benner, Steve Opsahl, and Brenda Black
Marine Science Institute, University of Texas at Austin, Port Aransas, Texas 78373

Tania Pimentel
Instituto Nacional de Pesquisas da Amazônia, 69,000 Manaus, Brazil

Jorge Quintanilla
Instituto de Investigaciones Quimicas, Universidad Mayor de San Andres, La Paz, Bolivia

Laurence Maurice
Institut de Recherche pour le Developpement (IRD), La Paz Bolivia

Abstract

We determined the concentrations and compositions of coarse particulate (>63 μm), fine particulate (0.1–63 μm), and dissolved (0.001–0.1 μm) organic matter collected along a river reach extending from a first-order stream in the Bolivian Andes, through the Beni River system, to the lower Madeira and Amazon Rivers. Dissolved organic carbon (DOC) concentrations increased down the total reach from ~80 to 350 μM. The percentage of total DOC with a molecular weight greater than ~1,000 atomic mass units that could be isolated by ultrafiltration also increased downstream from 40 to 80%. Weight percentages of organic carbon in the ultrafiltered isolates also grew downstream from 5% at the uppermost station to 37% in the Amazon mainstem. Organic carbon composed only 0.4–1.2 weight percentage of the total mass of the fine particulate fraction, which accounted for 70–80% of the total organic carbon (TOC) in transport through the highly turbid (~600–2000 mg L^{-1}) Beni sequence. Observed compositional differences were related primarily to the size fractions in which the organic matter occurred. On average, coarse particulate organic material exhibited an atomic C : N of 24, whereas ultrafiltered DOM was nitrogen poor, (C : N)a = 34, and fine particulate material was nitrogen rich, (C : N)a = 15. The lignin and stable-carbon isotopic compositions of these fractions indicate tree leaves and other nonwoody tissues from C3 land plants as predominant sources. Three molecular parameters demonstrate that the coarse, fine, and dissolved fractions of individual water samples are increasingly degraded downstream. Elemental nitrogen, amino acids, and basic amino acids are all preferentially associated with fine minerals. Observed geographical patterns included more positive $\delta^{13}C$ values in particulate organic matter from high altitude sites and an increase in the abundance and degradation of ultrafiltered dissolved organic matter down the drainage system. Many of these compositional patterns are imprinted within materials carried by low-order, high-altitude tributaries and appear to reflect processes occurring on the landscape.

[1] Corresponding author (jihedges@u.washington.edu).

Acknowledgments

We thank the University of Washington Marine Organic Chemistry Group, and Yves Gélinas and Ben van Mooy in particular, for comments on earlier drafts of this manuscript. Michael Peterson performed elemental analyses of inorganic colloidal materials isolated by ultrafiltration from Bolivian tributaries. The Bolivian Navy, as represented by Captain Alfonso Thames Crespo, generously provided laboratory space at the base in Riberalta. The first draft of this manuscript was completed while J.H. was a fellow of the Hanse Wissenschaftskolleg, Delmenhorst, Germany. We dedicate this paper to the memory of Néstor Abasto L., who lost his life sampling the Beni River on a subsequent expedition.

This is CAMREX publication 102.

Our research was funded by U.S. National Science Foundation grants DEB-9408676 and DEB-9815912.

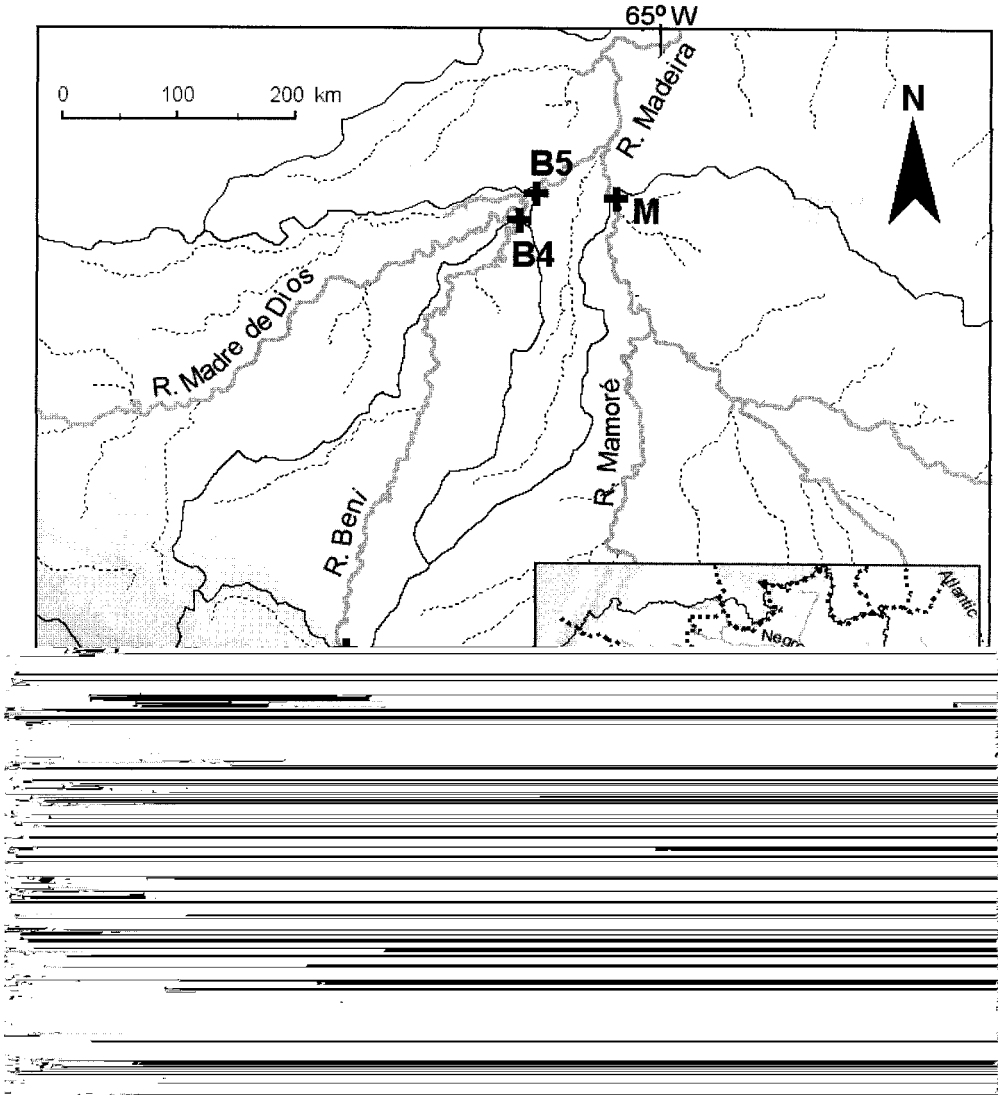

Fig. 1. Nested maps of upper South America showing sampling sites in the Bolivian tributaries and lower Madeira and Amazon Rivers (inset). Site symbols are listed in Table 1, along with other characteristics of the sampled regions. V and P indicate previous study sites in the lower mainstem at Vargem Grande and Manacapurú, respectively.

The concentrations (e.g., Meybeck 1982; Degens et al. 1991) and fluxes (Ludwig et al. 1996) of dissolved and particulate organic carbon (DOC and POC, respectively) in large rivers have been widely studied, and detailed time series have been reported for corresponding biochemical components from a small number of sites (Ittekkot and Arain 1986). In contrast, there have been only a few detailed tests (e.g., Depetris and Kempe 1993) of the predictions from the classic river continuum concept (Vannote et al. 1980; Minshall et al. 1985) that the size and degradation of dissolved organic matter should increase downstream, whereas the mean size of the particulate organic fraction should decrease. This scarcity of data is particularly true for large rivers, where the logistical challenge of collecting dissolved and particulate materials over an extended geographic area can be daunting. Because the river continuum concept was conceived almost 20 yr ago, largely on the basis of energetic and biological considerations for small streams and rivers, the extent to which these theoretical predictions parallel detailed molecular measurements of organic matter cycling within large rivers merits evaluation.

As a part of CAMREX (Carbon in the Amazon River EXperiment), we have been studying the forms and compositions of organic matter over a ~1,800-km reach (Fig. 1) of the Amazon River in Brazil (Richey et al. 1990; Devol and Hedges in press). A main focus in this study has been to representatively collect different size classes of organic matter being transported through the lower drainage system at various locations, seasons, and stages of the river hydrograph. These size fractions have then been analyzed for a

wide variety of chemical and isotopic compositions that reflect organic matter sources and processing. The present paper concerns parallel analyses of the same size fractions from a sequence of Andean tributaries that flow via the Rios Beni and Madeira into the lower Amazon (Fig. 1). These measurements provide an opportunity to investigate downstream patterns in organic matter composition within this dynamic stretch of the upper drainage network, as well as to compare these findings to previous results for the lower Madeira and Amazon sections. The latter ''full-basin'' perspective allows a test of river continuum concept predictions on an unprecedented physical scale.

Previous CAMREX studies (recently reviewed by Devol and Hedges in press) have shown that coarse particulate organic matter (CPOM $>$ 63 μm), fine particulate organic matter (FPOM = 0.1–63 μm), and dissolved organic matter (DOM) from the lower Amazon mainstem exhibit distinctly different bulk chemical (C:N, $\delta^{13}C$, and $\Delta^{14}C$) and biochemical (lignin, aldose, and amino acid) compositions. In contrast, the characteristic composition of each size fraction remains nearly constant throughout the year (and hydrograph) over the entire study reach (Hedges et al. 1986*a*, 1994). In brief, we have observed that CPOM chemically resembles sparingly degraded tree-leaf fragments (Hedges et al. 1994) and exhibits a ^{14}C content identical to contemporaneous atmospheric CO_2 (Hedges et al. 1986*b*). These relatively fresh sand-sized plant fragments are carried by wind and slope wash into the river within a few years of photosynthesis. In contrast, most FPOM in the lower Amazon appears to be adsorbed to the surfaces of mineral grains (Keil et al. 1997) and hence operationally falls into the size category of the smaller silt and clay particles with which it is associated. FPOM from the lower basin is more degraded than CPOM and is relatively enriched in nitrogen, amino acids, and basic amino acids. Although FPOM also derives primarily from tree leaves, it accumulates for decades to centuries on soil minerals before entering the river system via physical erosion (Hedges et al. 1986*b*). Parallel compositional patterns are exhibited between CPOM and FPOM fractions from major tributaries, including the Rio Madeira, where they discharge into the Brazilian Amazon (Hedges et al. 1986*a*, 1994).

DOM in the lower Amazon mainstem is compositionally distinct from both CPOM and FPOM, although it appears also to be derived largely from tree leaves (Hedges et al. 1994). Organic components of the dissolved fraction have been collected on two separate mainstem cruises, by use of two different methods. In the first field study (Ertel et al. 1986), dissolved humic substances were isolated from the mainstem and intervening tributaries by adsorption onto XAD-8 resin. The retained materials accounted for an average of 60% of the total DOC and were nitrogen depleted and more degraded than CPOM and FPOM fractions from the same water. High concentrations of bomb ^{14}C in both the humic- and fulvic-acid fractions isolated from the Rio Negro and lower Amazon mainstem indicated at least decadal lags between photosynthetic formation and riverine export (Hedges et al. 1986*b*). On a later cruise, dissolved organic matter in the size range of 1 nm–0.5 μm was recovered with a 1,000–atomic mass unit tangential-flow ultrafilter (Benner and Hedges 1993) from waters collected at the ends (Vargem Grande and Óbidos) and middle (Manacapurú, near Manaus) of the CAMREX study reach (Fig. 1). Six intermediate tributaries, including the Rios Negro and Madeira, were also sampled (Hedges et al. 1994). Ultrafiltered dissolved organic matter (UDOM) accounts for an average of 75% of the total DOC in these waters and thus includes a major portion of the previously studied humic fractions. UDOM isolates are more nitrogen-poor, oxygen-rich, and acidic than coexisting FPOM and CPOM fractions. Comparative analyses of the amino acid, carbohydrate, and lignin contents of all three sample types indicate that organic materials associated with smaller size fractions are consistently more degraded (Hedges et al. 1986*a*, 1994). This finding is consistent with the size-reactivity continuum model of Amon and Benner (1996), who demonstrated that smaller organic substances in the lower Amazon River exhibit poorer substrate quality. Thus, CPOM, FPOM, and UDOM fractions from the same samples exhibit distinctly different chemical compositions and dynamics within waters of the lower Amazon River system.

One explanation for these contrasting compositions and dynamics is that organic substances in the three different size categories share common biological sources but have been chemically altered and fractionated to varying extents in the process of microbial degradation and transport to the river system. Most vascular plant tissues photosynthesized in river drainage basins are biodegraded to soluble organic molecules $<$500 Da in size that are transported into microbial cells and respired. Solubilized organic remains that escape immediate respiration can be leached from the forest litter into soils, where they will partition between water and mineral surfaces. On the basis of laboratory and field studies, hydrophobic and/or nitrogen-rich organic substances should be preferentially immobilized by sorption onto soil minerals (Theng 1979; Hedges and Oades 1997), whereas more hydrophilic, nitrogen-poor molecules should remain dissolved and be carried via ground water to streams and rivers. Such continuous fractionation may lead to a type of ''regional chromatography'' (Hedges et al. 1994) by which sparingly soluble, nitrogen-rich organic substances are selectively retained within catchments. Given that FPOM and DOM together account for $>$90% to total organic carbon in the lower Amazon mainstream, biodegradation and partitioning together strongly influence the types and amounts of organic matter transport by the river. The compositional uniformity of organic matter throughout the 1,800-km study reach of the Brazilian mainstem suggests that the processes imprinting these distinct characteristics are active well upstream of the lower basin and could in large part occur on the landscape, as opposed to within the river channel.

This paper addresses the question of whether the compositions of organic materials carried within large river systems vary systematically downstream and, if so, in response to what natural processes? More specifically, do processes that imprint the compositions of bulk organic materials in river systems operate primarily within flowing waters (Vannote et al. 1980) and riparian zones (McClain et al. 1997), or do most alterations occur remotely on the landscape prior to introduction of allochthonous materials by groundwater and slope wash (Hedges et al. 1994)? This ''processor'' versus ''pipe'' distinction is critical to defining the time and

Table 1. Characteristics of the Bolivian river sampling sites.

River sampled	Sampling sites	Site code	Latitude (degrees S)	Latitude (degrees W)	Elevation (m_{asl})	DDS (km)	Water temperature (°C)	River depth (m)	FSS (mg L^{-1})	CSS (mg L^{-1})	DOC (μM)
Achumani	La Paz	B1	16° 30.40′	68° 01.82′	3,900	0	10.2	0.3	553	8	78
Alto Beni	Sapecho	B2	15° 33.71′	67° 22.41′	430	256	26.5	3.8	1,340	22	107
Beni	Rurrenabaque	B3	14° 32.22′	67° 29.53′	300	425	27.7	11.3	851	33	157
Beni	Riberalta-Arriba	B4	11° 00.88′	66° 06.18′	135	1,040	28.4	5.5	1,851	110	247
Beni	Riberalta-Bajo	B5	10° 48.05′	65° 57.68′	130	1,087	27.8	>11	1,048	264	229
Mamore	Guayaramerin	M	10° 50.18′	65° 18.55′	120	1,201	29.3	9.3	320	0.1	225
Madeira	28 km < Mouth	R	3° 32.50′	58° 54.80′	20	2,561	~28.0	~17.5	258	48	252
Amazon	Obidós	Z	1° 56.20′	55° 30.50′	10	3,026	~28.0	~50.3	174	29	346

Most field data are for the sampling period of 9–20 November 1994. Unless otherwise noted, data for the Rio Maderia and Amazon mainstem at Obidós are annual averages from at least eight seasonal samplings (e.g., Richey et al. 1986). Abbreviations: m_{asl}, meters above sea level; DDS, distance downstream from Achumani (GIS-based estimate); FSS, fine suspended solids; CSS, coarse suspended solids; DOC, dissolved organic carbon.

space scales over which rivers reflect their catchments and, hence, how drainage basins processes are best understood and managed. The organic compositional uniformity we have observed in previous studies of the lower Amazon River and its major tributaries may result primarily from sampling only higher-order reaches of the drainage network, where downstream contrasts are theoretically minimal (Vannote et al. 1980). If any segments of the Amazon system exhibit variable chemical characteristics, they should be lower-order streams and rivers in the Andean Cordillera (Minshall et al. 1985; Leopold 1994), whose organic components have been sparingly quantified (Guyot et al. 1992; Guyot and Wasson 1994) and remain uncharacterized in any detail.

We report here the first detailed biochemical analysis of organic matter from rivers in the Bolivian headwaters of the Amazon system, where the geomorphology of the catchments and the hydrology of their rivers change rapidly (Table 1). Organic materials were isolated during one sampling (9 November 1994–20 November 1994) from headwaters of the Rio Madeira (Fig. 1) and chemically characterized by essentially the same procedures used in previous CAMREX studies in the Brazilian lowlands. The concentrations of coarse, fine, and dissolved organic materials varied greatly along the upper portion of the ~3,000-km reach from near La Paz (3,900-m altitude) to the mouth of the Madeira (20 m) and onto Óbidos (10 m) in the lower mainstem. This geochemical snapshot demonstrates that many compositional aspects of the particulate organic fractions of the Bolivian tributaries closely parallel those of the lower mainstem, indicating a similar processing history. The corresponding dissolved organic component, however, exhibits distinct downstream trends in molecular weight and composition, which generally parallel predictions of the river continuum concept.

Study area

When the Bolivian tributaries were sampled in November 1994, water discharges were in the early rising stage of the hydrograph. The most upstream water sample was collected near La Paz in the Rio Achumani, within a kilometer or two of the river source (Sta. B1 in Fig. 1). At this point, the Achumani is a first-order stream ~50 cm wide and 10 cm deep. The next four samples were collected over a stretch of the Rio Beni that starts ~250 km downstream of Sta. B1 and continues ~1,100 km downstream to Sta. B5, just below the confluence with the Rio Madre de Dios. A sixth sample from this region was taken in the Rio Mamore, ~50 km upstream of its confluence with the Beni to form the Rio Madeira. The Mamore joins the Beni ~100 km downstream of Sta. B5 and hence does not have a compositional influ-

Table 2. Average geomorphological features of the river basins upstream of the Bolivian water sampling sites.

Site code	Area (km^2)	Slope (%)	Elevation (m_{asl})	% elevation >500 m	Area % sand	Area % clay	Soil % OC	Area % forest	Precipitation (mm yr^{-1})
B1	<100*	9.56	4,562	100.0	50.9	23.6	1.99	11.8	689
B2	29,540	13.70	2,728	99.6	76.8	12.5	0.71	28.2	959
B3	67,950	9.63	2,187	95.3	75.9	13.4	0.76	48.0	1,120
B4	118,000	5.77	1,369	57.6	54.7	29.2	0.72	58.9	1,480
B5	278,100	3.95	1,030	41.0	42.9	38.4	0.81	73.8	1,640
M	599,800	1.79	540	19.5	38.2	40.6	0.71	52.6	1,700
R	1,381,000	1.77	500	16.9	39.7	39.0	0.71	69.9	1,870
Z	4,677,000	1.60	453	15.3	37.5	38.5	0.72	78.6	2,150

Data are taken from different geographic information system sources (E. Mayorga, unpubl. data). Site codes are delineated in Table 2.

* The area of the Achumani basin upstream of sampling site B1 is too small to accurately determine. Weight percentages of soil organic carbon (%OC) are estimated from averages inventories (kg OC m^{-2}) within the upper meter and under the assumption of a soil bulk density of 1.65 g cm^{-3}. Sample site codes and abbreviations are as in Table 1.

ence on any of the upstream Bolivian samples (B1–B5). The Mamore drains a lower elevation region than the Beni, with average physical characteristics that more closely resemble those of the lower Madeira basin (Table 2). The locations, altitudes, and streambed distances between these six sites are given in Table 2, along with the temperatures and depths of the streams at the times of sampling. For comparison, corresponding average data from previous studies (Hedges et al. 1986*a*, 1994; Richey et al. 1990) are also tabulated for (1) the Rio Madeira just upstream from its confluence with the Amazon and (2) the lower Amazon mainstream at Óbidos, ~500 km downstream of the mouth of the Rio Madeira and 3,000 km downstream from Sta. B1 in the Bolivian highlands.

Methods

Sampling—Large-volume (100–200-liter) water samples were collected for organic analysis at all six Bolivian stations in Fig. 1. Water was composited from the shallow Rio Achumani (Sta. B1) by dipping. At the next two stations (B2 and B3), water samples were taken near the surface at midstream by use of a bucket. Large-volume water samples were collected at the three deeper sites (B4, B5, and M) with an electric pump submerged to 6/10 of the total river depth and directed into the current at midchannel. Coarse particulate material was separated by sieving onto a 63-μm Nitex screen, preserved with 50-μM concentration of $HgCl_2$ biocide, and oven dried at ~30°C. The sand-free water was then passed through an Amicon DC-10 ultrafilter system fitted with an Amicon H5MP01–43 hollow-fiber cartridge with a nominal 0.1 μm cutoff size, to isolate fine particles. The retained particles were recovered when the volume of suspension remaining in the ultrafilter reservoir reached ~1.5 liters. The resulting 2 liters of suspension was then adjusted to 50 μM in $HgCl_2$. High-molecular-weight dissolved material that permeated the 0.1-μm filter cartridge was recovered with tandem Amicon S10-N1 tangential flow ultrafilters with a nominal cutoff size of 1,000 atomic mass units, corresponding roughly to 0.001 μm (Benner 1991). This concentrate was reduced to ~1-liter volume and adjusted to 50 μM in $HgCl_2$. Both of the ultrafilter isolates from each site were concentrated and dried in a Savant centrifugal evaporator (Hedges et al. 1994).

Smaller (~10 liters) depth-integrated, discharge-weighted water samples were collected at all sites except B1 (too shallow) with the same type of collapsible-bag apparatus (Nordin et al. 1983) that was used previously in the lower Amazon mainstream (Richey et al. 1986). The smaller Bolivian rivers, however, were sampled at three evenly spaced points across the channel by use of a hand winch operated from a small anchored boat. The three samples were composited and subsampled for measurements of total suspended solids (TSS) and DOC, as described in Richey et al. (1986, 1990). Concentrations of fine suspended solids were determined gravimetrically by filtering triplicate aliquots of depth-integrated water samples onto separate 0.45-μm Millipore HAWP filters. Concentrations per unit volume of coarse and fine particulate materials and their organic components were determined on the basis of sieved and Millipore-filtered masses, respectively.

Chemical analyses—Most chemical analyses were made as described by Hedges et al. (1986*a*, 1994). Weight percentages of organic carbon (%OC) and total nitrogen (%TN) were measured after vapor phase acidification by use of a Carlo Erba model 1108 CHN analyzer (Hedges and Stern 1984). This method has a precision of approximately ±2%. Stable carbon and nitrogen isotope compositions were determined by sealed-tube combustion with typical precisions (for both) of ±0.2‰ (Quay et al. 1992). Stable isotope compositions are reported as the per mil relative variation ($\delta^{13}C$ and $\delta^{15}N$) from the Pee Dee Belemnite (PDB) and atmospheric N_2 standards, respectively. DOC concentrations were measured on acidified/purged samples with an average precision of ±5% by use of a Shimadzu TOC-5000 high-temperature catalytic oxidation analyzer (Benner and Hedges 1993). All samples were analyzed by triplicate injection versus potassium hydrogen phthalate standards and corrected for the system blank (Benner and Strom 1993). This DOC method has been confirmed by comparison with CHN analysis (Benner and Hedges 1993).

Aldoses were analyzed by the method of Skoog and Benner (1997). Dry samples were pretreated with 12 M H_2SO_4 for 2 h at room temperature, diluted to 1.2 M H_2SO_4, and hydrolyzed for 3 h at 100°C. After neutralization with $CaCO_3$, hydrolysate solutions were deionized with mixed anion/cation resins and degassed with He. The resulting solutions were analyzed with a Dionex 500 ion chromatograph fitted with a PA-1 column and a pulsed amperiometric detector. The hydrolysate mixture was eluted isocratically with a 24-mM solution of NaOH. Individual aldoses were measured with precisions of ±5–30%, depending on their relative amount and chromatographic resolution from other mixture components.

Amino acids were analyzed by high-pressure liquid chromatography by use of charged-matched recovery standards (Cowie and Hedges 1992*a*). Aqueous hydrolyses were done under N_2 for 70 min at 150°C. The hydrolysis mixture was dried and dissolved in water, and component amino acids were converted to fluorescent *o*-phthaldiahyde derivatives within a Gilson model 231 automated injector. The *o*-phthaldiahyde derivatives were immediately injected onto a 15 cm × 4.6–mm inner diameter (i.d.) column operated in reverse phase mode with 5-μm C_{18} packing. By this method, individual amino acids were measured with precisions of ±5–10%.

Lignin phenols were measured as described by Opsahl and Benner (1995, 1997). Solid samples were reacted with a suspension of CuO in 8 wt% NaOH within a high-pressure bomb at 155°C (internal temperature). Reaction products were converted to trimethylsilyl derivatives and analyzed on a Hewlett Packard 5890A gas chromatograph fitted with an HP-5MS capillary column (30 m × 0.24 mm i.d.) and operated with He carrier gas. Trimethylsilyl derivatives of individual phenolic products were identified with a Hewlett Packard 5972 mass selective detector and quantified by selective ion monitoring. The precision of this method was also ±5–10%.

Basin chacterizations—River site and basin characteristics (Table 1) were calculated by use of the ArcInfo (ESRI 1997) Geographical Information System. Latitude and longitude coordinates of the sampling sites were recorded in the field using a global positioning system unit and then imported into ArcInfo, where they were matched to the nearest point on the Digital Chart of the World digitized river channels dataset (Danko 1992). To delineate basin boundaries and calculate areas draining to the sampling points, the Digital Chart of the World rivers were first converted from vectors to a raster map at 0.005° (~500 m) resolution. Geographical Information System algorithms were then developed to allocate all 0.005° cells in the raster map to the nearest river cell (Sekulin et al. 1992) and to calculate distances along the river channels. Mean basin properties were computed by use of raster data sets regridded to a common resolution of 0.01° (~1 km) and take into account the variation of actual pixel area (km^2) with latitude. Basin averages for continuous variables such as elevation were calculated as the mean of all cell values in the drainage area. Classed variables (forested pixels and pixels at elevation >500 m) represent the percentage of the basin covered by cells of the corresponding class.

Mean basin elevation (in meters), the fraction of the basin above 500 m elevation, and mean basin slope (%) were calculated by use of the GTOPO30 30-s (~1 km) elevation data set (Gesch et al. 1999). Mean basin sand and clay fractions (%) were used as proxies for soil mineral surface availability. For Brazilian areas, the EMBRAPA (1981) soil map was combined with RADAMBRASIL (1984) soil profile data to calculate mean values for the upper 1 m of soil. Outside of Brazil, the Zobler 1° data set was used (Staub and Rosenzweig 1992), under the assumption that the upper 30 cm of soils were representative of the upper 1 m. Soil organic carbon (OC) content was calculated as OC stocks to 1-m depth, under the assumption of a soil bulk density of 1.65 g cm^{-3}. Within Brazil, the EMBRAPA soil map was combined with soil OC values for the upper 1 m, calculated from RADAMBRASIL (Moraes et al. 1995). Outside Brazil, a 0.5° map of Holdridge bioclimatic life zones (Holdridge 1947; Leemans 1992) was combined with a soil OC data set classified by Holdridge life zones (Post et al. 1982, 1985). Percentage of forest versus nonforest vegetation cover was estimated with an 8-km vegetation map derived from 1980s satellite data (Stone et al. 1994). Mean rainfall patterns were represented by basin averages of mean annual precipitation (in mm). Mean monthly rainfall maps were obtained by interpolating and summing several hundred rain gauges with daily data from 1983–1989 (H. Greenberg et al. unpublished).

Results

The physical characteristics of the water samples and their collection sites (Table 2) are most variable in the upper portion of the Bolivian sequence, in part because of the precipitous drop in the stream network as it exits the high Andes (Table 1, Fig. 2a). Only the uppermost (Achumani) water sample came from a site with an elevation (3,900 m) that is >500 m, a channel depth of <1 m, and from water temperatures (10.2°C) appreciably <26°C. Many of the geomorphological features of the sampling sites change less abruptly, however, when viewed on the basis of the average characteristics of the drainage basin integrated over all the area which the sampled waters drain (Table 2). This more appropriate cumulative perspective reflects a rather smooth exponential decrease in the average altitudes of areas drained by sequential sampling sites (Fig. 2a). The average slopes of the sampled basin areas maximize near 14% at Sta. B2 in the Alto Beni and then also drop exponentially to values near 2% in the lower Madeira and Amazon (Fig. 2b). Integrated percentages of sampled catchment areas covered by forest and characterized by finer textured soils also increase downstream, as does average precipitation (Table 1). Whether integrated or not, most of the variability observed in each physical and geomorphic characteristic of the sampled catchments occurs along the ~1,100-km segment of the Bolivian river network (Tables 1, 2), where maximal corresponding

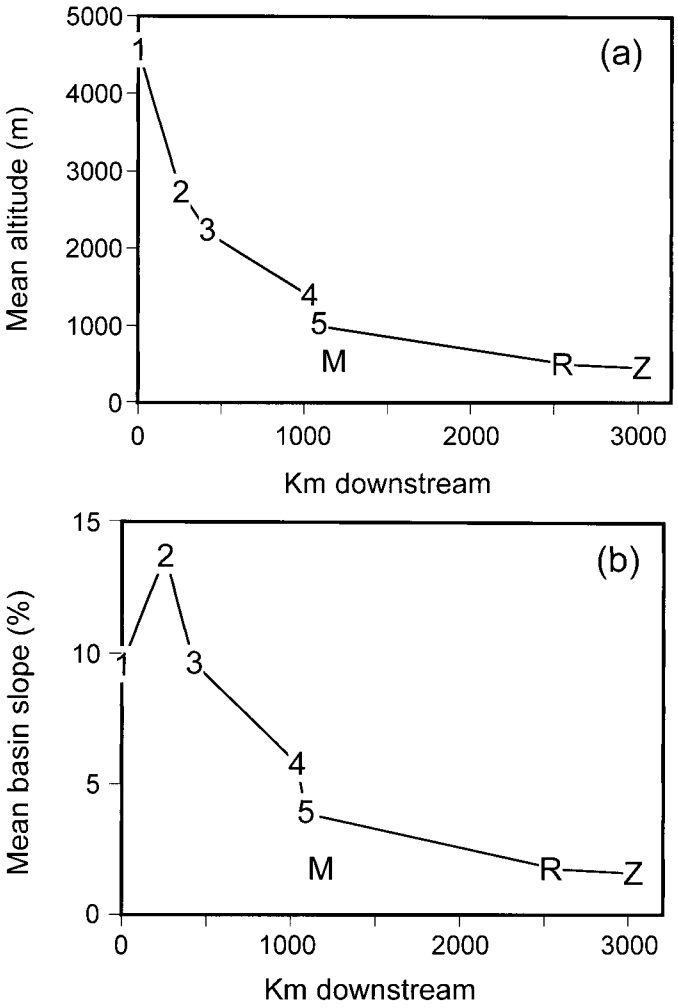

Fig. 2. Plots versus kilometers downstream in the study reach of: (a) mean basin altitude; and (b) mean basin slope. *See Table 1* for sample symbols and Table 1 for other average basin properties. In this and following plots, the Rio Mamore (M) sample is assigned the distance downstream where this separate river joins the Rio Beni but is not included in corresponding trend lines for the study reach.

Table 3. Organic carbon and nitrogen distributions and compositions.

Sample site	Size fraction	Sample symbol	OC (wt %)	TN (wt %)	C/N atomic	OC (μM)	TOC (%)	δ^{13}C (‰)	δ^{15}N (‰)
B1	CPOM	C1	0.35	0.09	4.5	2	0.9	−25.0	2.9
B1	FPOM	F1	0.37	0.15	2.8	172	68.1	−24.2	2.7
B1	UDOM	D1	4.80	0.30	18.7	32	12.8	−27.0	1.8
B2	CPOM	C2	3.70	0.20	21.8	67	4.7	−26.7	2.5
B2	FPOM	F2	1.11	0.16	8.2	1,240	87.7	−25.5	5.4
B2	UDOM	D2	10.3	0.47	25.6	54	3.8	−27.2	2.6
B3	CPOM	C3	1.84	0.09	23.7	51	4.6	−28.2	1.9
B3	FPOM	F3	1.26	0.16	9.5	894	81.1	−26.9	4.4
B3	UDOM	D3	16.2	0.62	30.5	73	6.6	−28.8	2.2
B4	CPOM	C4	0.29	0.05	6.3	26	2.4	−27.4	3.4
B4	FPOM	F4	0.55	0.10	6.2	845	75.5	−26.7	4.5
B4	UDOM	D4	24.8	0.97	29.7	137	12.2	−25.7	4.3
B5	CPOM	C5	0.25	0.05	6.2	55	5.9	−27.5	3.6
B5	FPOM	F5	0.74	0.13	6.9	644	69.4	−27.5	4.5
B5	UDOM	D5	21.9	0.96	26.8	151	16.3	−28.3	2.1
M	CPOM	CM	3.80	0.20	22.0	0	0.1	−25.8	ND
M	FPOM	FM	0.78	0.13	6.9	207	47.9	−26.4	4.3
M	UDOM	DM	16.2	0.72	26.4	90	20.8	ND	2.0
R	CPOM	CR	0.84	0.04	25.7	34	6.6	−27.4	ND
R	FPOM	FR	0.96	0.14	8.2	206	40.6	−26.6	4.9
R	UDOM	DR	28.6*	1.20*	27.9*	208*	40.9†	−28.0*	3.1*
Z	CPOM	CZ	1.00	0.06	20.2	24	4.2	−28.0	ND
Z	FPOM	FZ	1.21	0.14	10.0	175	30.7	−27.0	5.4
Z	UDOM	DZ	36.7*	1.26*	34.1*	264*	46.3†	−29.2*	4.0*

Unless otherwise noted, data for the Rio Madeira and Amazon mainstem at Óbidos are annual averages for at least eight seasonal samplings (e.g., Richey et al. 1986).

* Data are from only CAMREX XII (April–May 1990).

† UDOM from CAMREX XII added to average CPOM and FPOM from earlier cruises.

Abbreviations: CPOM, coarse particulate organic matter; FPOM, fine particulate organic matter; UDOM, ultrafiltered dissolved organic matter; OC, organic carbon, TN, total nitrogen (including inorganic N); % TOC, percentage of total organic carbon (the latter including total DOC); δC^{13} and δN^{15} are the per mil deviations of the $^{13}C/^{12}C$ and $^{15}N/^{14}N$ of the samples from the same ratios for the PDB and atmospheric N_2 stable isotope standards, respectively; ND, not determined. Other abbreviations and symbols are as in Table 1.

changes in organic matter concentrations and compositions would be expected.

The concentration of bulk coarse (>63 μm) suspended solids increased steadily from 8–264 mg L^{-1} from the Achumani to the lower Beni sampling sites (Table 1). Fine (0.1–63 μm) suspended solids increased from 550–1,340 mg L^{-1} between B1 and B2 and then remained >850 mg L^{-1} throughout the Beni system. At the time of sampling, the lower Mamore carried 320 mg L^{-1} of fine solids and essentially no sand from its relatively low-relief basin (Table 1). Concentrations of coarse and fine particles dropped from 48 and 258 mg L^{-1} at the mouth of the Madeira to 29 and 174 mg L^{-1} at Óbidos, respectively.

Concentrations of TOC and its distributions among the coarse, fine, and dissolved size fractions (Table 3) varied markedly through the 3,000-km reach (Fig. 3). TOC increased sharply from ~250 μM at Achumani, to almost 1,500 μM, at the next downstream station (B2). TOC dropped with basin slope (Table 2) to ~500 μM within the Beni reach (B2–B5) and by a comparable amount, to concentrations of ~500 μM, at the mouth of the Madeira and within the lower Amazon. The major determinant of these trends was the concentration of carbon in the fine size fraction, which maximized at ~1,250 μM at B2 and accounted for >60% of TOC throughout the Beni reach. In comparison, FPOM accounted for <210 μM of organic carbon in the Mamore, Madeira, and Óbidos water samples, corresponding to less than half of the corresponding TOC values. Concentrations of OC in the coarse size fraction never exceeded 70 μM or 7% of the TOC in any sample. Total DOC concentrations increased steadily downstream and with altitude (Fig. 4a), from a low of 78 μM at Achumani to values of 225–250 μM in the lower Beni, Mamore and Madeira. A mean DOC concentration of ~350 μM was observed at Óbidos, equivalent to >70% of TOC in transport at this point in the lower Amazon. The higher-molecular-weight fraction of DOC that could be isolated by ultrafiltration with a ~1-nm pore-size membrane also increased steadily downstream (Fig. 4b), from 40% at the uppermost Achumani sample to near 60% at the bottom on the Beni (B4 and B5) and 80% in the lower Madeira and Amazon reaches.

%OC in the coarse fractions varied between 0.25 and 3.8 (Table 3), with the highest values observed at B2 and in the Rio Mamore. Given that organic matter averages ~50 %OC, inorganic material composed at least 90% of the total mass of the collected sand-size particles. The corresponding fine particle fractions contained 0.37–1.26 %OC and thus comprised >97% inorganic material. There was no evident distribution pattern in the %OC of this silt : clay fraction. A plot of %OC versus %TN for the coarse and fine size fractions

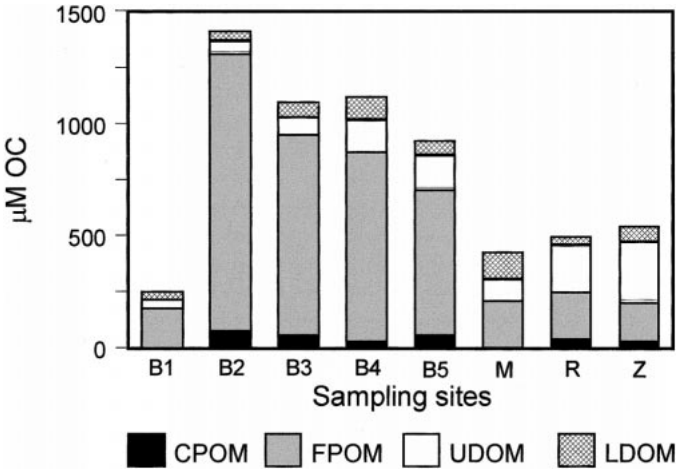

Fig. 3. Organic carbon concentrations (μM) in the coarse (CPOM), fine (FPOM), ultrafiltered dissolved (UDOM), and low-molecular-weight dissolved (LDOM) fractions of water samples collected along the study reach (*see* text for size ranges and Table 1 for site codes).

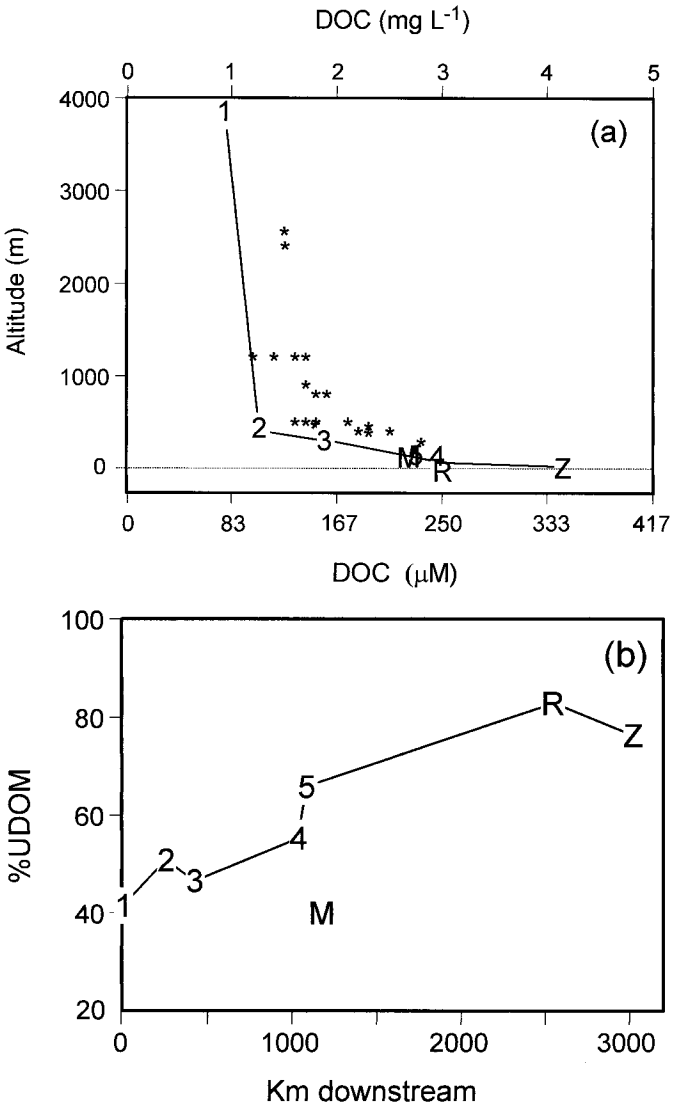

Fig. 4. Frame (a) illustrates dissolved organic carbon concentration plotted versus altitude at the water collection sites (Table 1). Asterisks indicate corresponding data from Guyot and Wasson (1994) for the Rio Beni system. Frame (b) shows the percentage of total DOC that was recovered in the ultrafiltered (UDOM) fraction of the water samples in Table 1.

(Fig. 5a) shows the usual direct relationship of the two elemental abundances. Both the coarse and fine Achumani samples, however, contained unusually high concentrations of total nitrogen for their organic carbon contents and (when converted to atom equivalents) exhibited quite low atomic C : N ratios, (C : N)a, of 4.5 and 2.8, respectively. The elemental data for the other seven coarse samples gave an excellent fit ($r^2 = 0.95$) to a straight line, with a small positive nitrogen intercept and a slope corresponding to a (C : N)a of 24. Elemental data for the seven samples of fine suspended sediment (excluding F1) produced a good fit to a straight line ($r^2 = 0.81$), with a slope corresponding to (C : N)a of 15 (Fig. 5a). The intercept of the correlation line near 0.06 %TN indicates that one-half to one-third of the bulk nitrogen in these fine particle mixtures is inorganic. Thus the slope-derived (C : N)a of the fine particulate samples (~15) should reflect their organic component more closely than the corresponding numeric average (~8).

The elemental compositions of the corresponding UDOM exhibited surprising downstream trends (Fig. 5b). The UDOM isolate from the Rio Achumani head waters had an extremely low %OC near 5% and thus consisted of ~90% inorganic matter. This component could not have been dissolved simple ions, which efficiently pass through the 1-nm pores of the ultrafilter (Benner 1991) and thus appears to be colloidal mineral. Cursory elemental analysis of the inorganic component of this isolate (by ICPMS) shows it to be aluminosilicate in nature. The organic concentrations of the UDOM isolates increased progressively downstream, to %OC values near 25% at the bottom of the Beni section, 30% in the lower Madeira, and 35% at Óbidos. Overall, %TN closely paralleled %OC ($r^2 = 0.96$), with a slope corresponding to a (C : N)a of 34. This line also extrapolates to a positive %TN intercept (Fig. 5b), possibly resulting from inorganic nitrogen associated with colloidal minerals predominating in higher-altitude samples. Dissolved organic matter thus becomes larger in effective size (Fig. 4b) as the concentration of colloidal inorganic particles decreases downstream (Fig. 5b).

The stable carbon isotopic compositions of all three size fractions also varied with distance downstream (Fig. 6a) and hence altitude (Table 3). The $\delta^{13}C$ values of the organic carbon in all three size fractions decreased by 2–3‰ among the first three stations (B1–B3), over a corresponding drop in mean basin elevation of ~2,400 m (Table 2). Little additional change in $\delta^{13}C$ was observed further downstream in any size fraction, except for an abrupt increase to −25.7 % for UDOM from Sta. B4. In contrast, $\delta^{15}N$ generally increased downstream in both the FPOM and UDOM fractions (Fig. 6b), with no apparent trend (due in part to limited data) for CPOM. Overall, FPOM from a given water sample was

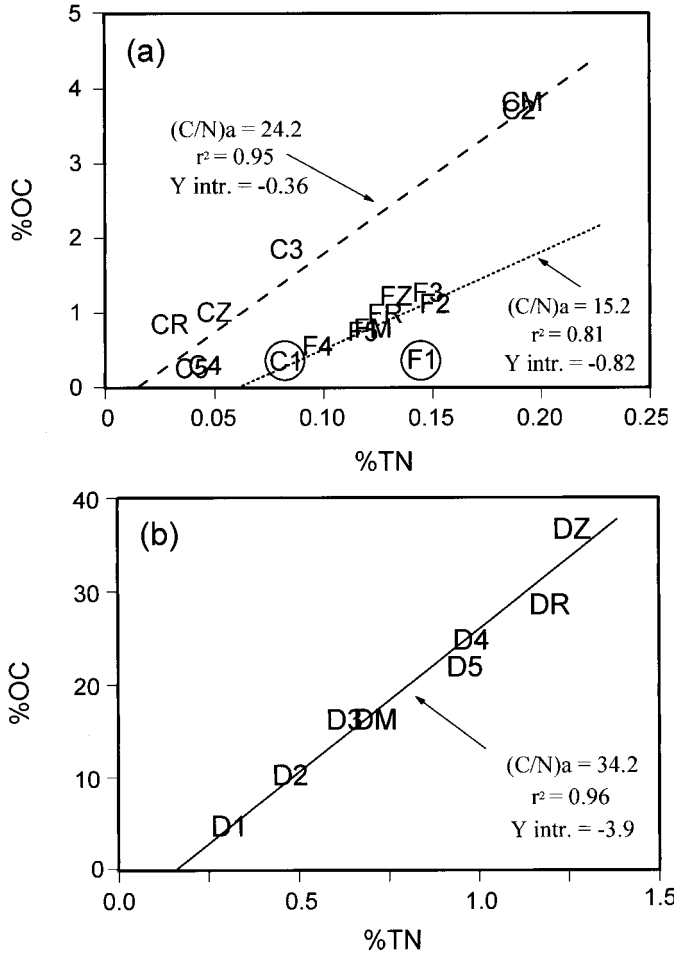

Fig. 5. Weight percentage organic carbon (%OC) versus weight percentage total nitrogen (%TN) for: (a) the coarse (C) and fine (F) particulate size fractions and (b) the corresponding ultrafiltered dissolved (UDOM) isolates (D). Values in the boxes are for straight lines giving the best least-squares fit to the data, except for the two circled particulate samples from Sta. 1. *See Table 1* for site codes following the previous sample fraction symbols.

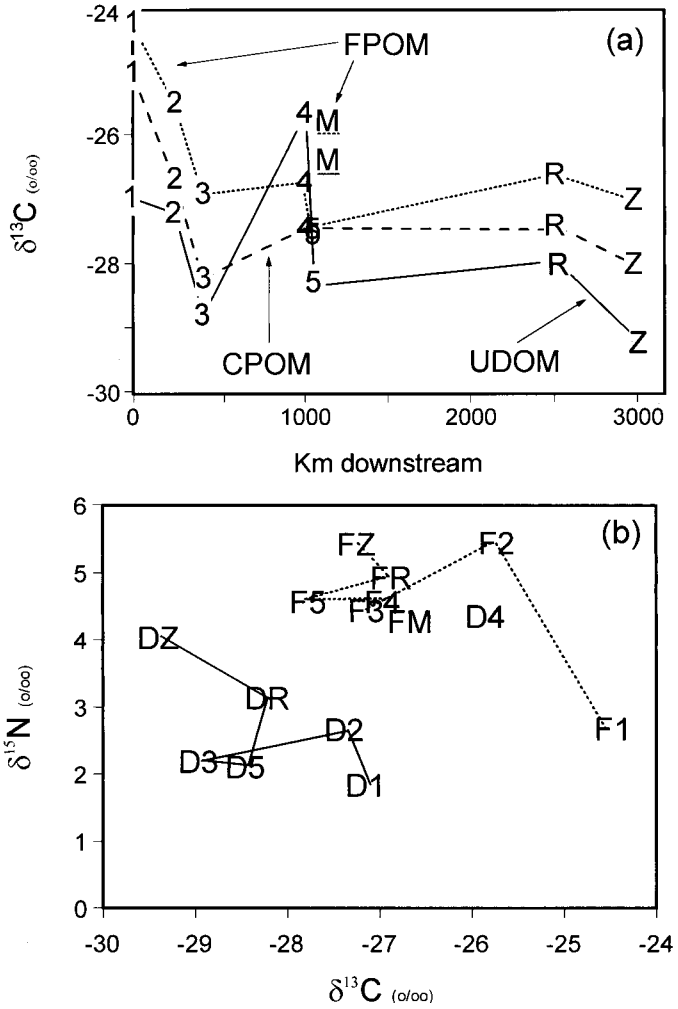

Fig. 6. Frame (a) illustrates stable carbon isotopic compositions (as $\delta^{13}C$ in per million versus PDB) of organic carbon in the three size fractions collected at increasing distances downstream of Achumani. Frame (b) shows a plot of $\delta^{13}C$ versus $\delta^{15}N$ for ultrafiltered dissolved (UDOM) and fine dissolved (FPOM) samples from the same stations (D4 has not been linked with the other UDOM data points).

enriched by 1–3‰ in both ^{13}C and ^{15}N versus the coexisting UDOM, creating the offset parallel lines in Fig. 6b.

Organic carbon–normalized yields of lignin, aldoses, and amino acids from the six sets of Bolivian samples showed no clear pattern with distance downstream (Tables 4–6). Yields of total lignin–derived phenols (Λ, mg [100 mg OC]$^{-1}$) generally decrease from a range of 5.7–9.3 for CPOM to 0.5–1.8 for FPOM and 0.5–1.2 for UDOM. Corresponding yields of total aldoses (TCH_2O, mg [100 mg OC]$^{-1}$) follow a similar trend (CPOM = 6.0–20; FPOM = 3.2–5.8; and UDOM = 1.2–2.0), without any overlap in yield between FPOM and UDOM. Total amino acid yields (mg [100 mg OC]$^{-1}$) are comparable between the coarse and fine fractions (7.3–17) of the Andean tributary samples, which gave substantially more amino acid than the corresponding UDOM isolates (3.9–5.6). This general pattern of decreasing yield of biochemicals from increasingly smaller size fractions is similar to that seen in the lower Rio Madeira and throughout the mainstem (Table 4; Hedges et al. 1986*a*, 1994). Compositional trends within these three biochemical classes will be selectively treated in the following discussion, since they pertain to organic matter sources and processing.

Discussion

The following discussion will address four major questions: (1) what factors affect distributions of coarse, fine, and dissolved organic materials at sequential collection sites in these Bolivian tributaries; (2) what are the apparent sources of organic matter in the three nominal size fractions; (3) to what extent do the organic materials in these isolates appear to have been degraded; and (4) is there evidence for selective partitioning of the component organic molecules between particulate and dissolved forms? Each of these discussions will include evaluations of downstream trends that ultimately

Table 4. Average* lignin phenol yields, in mg (100 mg OC)$^{-1}$, from individual riverwater size fractions.

Site	Fraction	VAL	VON	VAD	SAL	SON	SAD	CAD	FAD	Λ
B1	CPOM	ND	ND	ND	ND	ND	ND	ND	ND	ND
B1	FPOM	0.162	0.021	0.080	0.097	0.029	0.025	0.015	0.029	0.453
B1	UDOM	0.176	0.020	0.100	0.097	0.028	0.024	0.010	0.012	0.468
B2	CPOM	1.596	0.499	0.479	1.566	0.477	0.446	0.382	0.445	5.89
B2	FPOM	0.358	0.105	0.135	0.256	0.080	0.073	0.040	0.120	1.17
B2	UDOM	0.291	0.118	0.206	0.138	0.090	0.092	0.028	0.033	0.997
B3	CPOM	2.232	0.876	0.875	2.826	0.792	0.824	0.401	0.422	9.25
B3	FPOM	0.576	0.155	0.222	0.441	0.121	0.121	0.047	0.046	1.73
B3	UDOM	0.336	0.156	0.338	0.078	0.095	0.110	0.033	0.025	1.17
B4	CPOM	1.504	0.399	0.463	1.473	0.401	0.381	0.155	0.113	4.89
B4	FPOM	0.379	0.126	0.200	0.268	0.100	0.105	0.027	0.024	1.23
B4	UDOM	0.264	0.181	0.218	0.072	0.067	0.079	0.035	0.009	0.925
B5	CPOM	1.752	0.496	0.512	1.782	0.466	0.404	0.156	0.144	5.71
B5	FPOM	0.547	0.161	0.247	0.488	0.139	0.137	0.042	0.028	1.79
B5	UDOM	0.262	0.227	0.256	0.172	0.086	0.107	0.021	0.012	1.14
M	CPOM	ND	ND	ND	ND	ND	ND	ND	ND	ND
M	FPOM	0.272	0.108	0.153	0.210	0.089	0.085	0.035	0.031	0.975
M	UDOM	0.217	0.136	0.168	0.039	0.052	0.071	0.040	0.011	0.731
R	CPOM	2.293	0.525	0.527	1.807	0.459	0.343	0.187	0.127	6.27
R	FPOM	0.445	0.138	0.213	0.433	0.128	0.100	0.054	0.050	1.56
R	UDOM	0.352	0.147	0.390	0.245	0.132	0.201	0.068	0.064	1.28
Z	CPOM	2.134	0.489	0.491	1.753	0.449	0.351	0.149	0.103	5.92
Z	FPOM	0.486	0.149	0.228	0.450	0.141	0.135	0.046	0.045	1.68
Z	UDOM	0.296	0.120	0.359	0.170	0.088	0.164	0.039	0.041	1.60

* FPOM data for the Rio Madeira and Amazon mainstem at Óbidos are for one sampling during CAMREX XII (April–May 1990). The corresponding CPOM and FPOM data are for no more than three samplings during CAMREX II–IV (August 1982–March 1983). Abbreviations: VAL, vanillin; VON, acetovanillone; VAD, vanillic acid; SAL, syringaldehyde; SON, acetosyringone; SAD syringic acid; CAD, *p*-coumaric acid; FAD, ferulic acid; Λ, total yield, also in mg (100 mg OC)$^{-1}$, of the eight previously listed lignin phenols. All other abbreviations and symbols are as in Tables 1 and 3.

tie into the extensive data set for the lower Madeira and Amazon mainstem (Fig. 1) and pertain to the fundamental issue of whether organic matter compositions evolve downstream. When informative, comparisons also will be made to measurements obtained by other groups in the Amazon drainage network and other river systems. The following discussion is based solely on water compositions observed during a single low-water sampling period (November 1994). Because extents of temporal variation in this study area can be substantial (Guyot et al. 1988), the following discussion pertains at present only to the observed state of the Beni system at this one point in time. A synthesis of these concepts within the perspective of the river continuum concept will be presented in the following overview.

Distributional trends—The extents to which the concentrations and bulk compositions of the different organic fractions (Table 3) correlate with each other and with characteristics of the upstream catchment (Table 2) were appraised by applying Spearman nonparametric statistics (at the 95% confidence level) to data for each of the three size classes. The DOC concentrations in Table 2 were negatively correlated with the altitude of the sampling site and positively correlated with the %TN, (C : N)a of the dissolved fraction, and the average percentage of forest coverage upstream of the water sampling site. Correlations of DOC with average catchment slope and area percentage of sand were appreciable (>90%) but not significant. The observed pattern of increasing DOC concentration with decreasing altitude at the sampling site (Fig. 4a) is the same as reported by Guyot and Wasson (1994) for a much more detailed survey of DOC in waters of the Beni system. In both studies, DOC concentrations increase abruptly as the river flows down onto the floodplain (llanos) that extends at an altitude of ~150 m between the Andean piedmont and the Brazilian shield. True to this pattern, the Achumani sample (B1 in Fig. 1) is higher in altitude and lower in DOC than any sample from the region reported by Guyot and Wasson (1994). Although our DOC values run slightly lower at a given altitude than in the previous study, this small difference may result from our November collections being at a time of lower discharge and DOC concentration (Guyot and Wasson 1994). These authors attribute elevated DOC concentrations in the lower river system to increased contributions from fringing floodplains. As would be expected based on their mountainous setting (Meybeck 1982), DOC concentrations (80–250 μM) measured in the Beni system fall within the lower range of values for rivers of the world.

Concentrations of FPOM (Fig. 3) varied in the same form as average basin slope (Fig. 2b) but were not significantly correlated with this or any other variable. Concentrations of CPOM (Fig. 3) were not correlated significantly with FPOM or any other measured variable. Because we do not have synoptic discharge data, it is not possible to convert these concentration data to corresponding fluxes for comparison to other flux-based relationships (e.g., Ludwig et al. 1996). Larger data sets with proportionately greater representation

Table 5. Aldose yields, in mg (100 mg OC)$^{-1}$, from individual riverwater size fractions.

Site	Fraction	ARA	XYL	RHA	FUC	MAN	GAL	GLC	TCH_2O
B1	CPOM	0.53	1.68	0.13	0.07	0.26	0.47	3.74	6.88
B1	FPOM	0.48	0.46	0.47	0.23	0.77	0.87	1.30	4.57
B1	UDOM	0.13	0.17	0.28	0.15	0.22	0.16	0.53	1.62
B2	CPOM	1.99	4.07	0.68	0.27	1.35	2.13	10.53	20.9
B2	FPOM	0.58	0.54	0.48	0.22	1.04	0.99	2.23	6.09
B2	UDOM	0.16	0.24	0.34	0.18	0.30	0.27	0.48	1.97
B3	CPOM	1.77	3.55	0.64	0.25	1.33	1.91	10.63	20.1
B3	FPOM	0.63	0.60	0.47	0.19	0.89	0.93	2.07	5.77
B3	UDOM	0.11	0.13	0.19	0.11	0.21	0.16	0.28	1.19
B4	CPOM	0.92	1.21	0.38	0.15	0.58	0.88	3.84	7.96
B4	FPOM	0.36	0.23	0.26	0.09	0.45	0.43	0.77	2.59
B4	UDOM	0.11	0.16	0.24	0.15	0.18	0.17	0.25	1.25
B5	CPOM	0.89	1.32	0.34	0.16	0.68	0.86	4.10	8.36
B5	FPOM	0.55	0.44	0.43	0.16	0.73	0.68	1.46	4.44
B5	UDOM	0.13	0.22	0.28	0.14	0.37	0.23	0.46	1.82
M	CPOM	0.87	1.97	0.20	0.18	0.56	0.85	7.33	12.0
M	FPOM	0.37	0.30	0.41	0.20	0.55	0.52	0.87	3.22
M	UDOM	0.14	0.20	0.27	0.24	0.22	0.23	0.30	1.60
R	CPOM	ND	ND	ND	ND	ND	ND	ND	ND
R	FPOM	0.83	0.59	0.88	0.30	1.83	1.14	3.20	8.78
R	UDOM	0.38	0.47	0.62	0.36	0.54	0.59	0.97	3.92
Z	CPOM	1.89	1.91	0.62	0.21	1.32	1.79	8.05	15.8
Z	FPOM	1.06	0.83	0.86	0.45	1.75	1.38	3.78	10.1
Z	UDOM	0.27	0.32	0.50	0.26	0.39	0.41	0.65	2.79

Rio Madeira and Amazon data are for one sampling April–May 1994 (Hedges et al. 1994). Abbreviations: ARA, arabinose; XYL, xylose; RHA, rhamnose; FUC, fucose; MAN, mannose; GAL, galactose; GLC, glucose; TCH_2O, total aldose yield (excluding lyxsose and ribose). All other abbreviations and symbols are as in Tables 1 and 3.

of high altitude samples will be necessary to link organic distributions within these size fractions to basin properties.

Organic sources—Given the large gradients in geomorphology, climate, and vegetation along the first 1,100-km reach of the Beni drainage system (Tables 1, 2), the corresponding contrasts in biochemical and isotopic compositions within individual size classes are often small. One exception to this general uniformity is the previously noted trend toward more positive $\delta^{13}C$ values among all organic fractions from higher altitudes (Fig. 6). A similar systematic increase in $\delta^{13}C$ with altitude has been noted for particulate materials from Peruvian tributaries of the Amazon River, with $\delta^{13}C$ values as positive as -24.5‰ reported for the upper reaches of the Huigueras River (Cai et al. 1988). Similar increases on the order of 0.75‰ and 1.0‰ per 1,000 m of altitude, respectively, also have been noted by Bird et al. (1994) for soils from New Guinea and by Körner et al. (1988) for leaves of C3 plants. This agreement and the generally parallel downstream trends in $\delta^{13}C$ among the relatively fresh CPOM and more degraded FPOM and UDOM fractions points toward an altitudinal effect (Quay et al. 1992). Other factors, however, probably lead to the ~1‰ offsets in $\delta^{13}C$ among coexisting FPOM (more positive), CPOM (intermediate), and UDOM (more negative) fractions along the entire study reach (Fig. 6a).

An Andean source of ^{13}C-rich particulate organic matter in the Amazon River system was previously inferred by Quay et al. (1992) on the basis of geographic and discharge trends in the Brazilian mainstem. Under the assumption that the most positive $\delta^{13}C$ value (-26.8‰) measured in the Brazilian mainstem and Rio Madeira represents a high-altitude endmember, these authors conservatively estimated that >35% of the FPOM suspended in the lower Amazon (at Óbidos, $\delta^{13}C = -27.4$‰) is of lowland origin ($\delta^{13}C = -28.5$‰). Given the more positive $\delta^{13}C$ values (near -25.5‰) reported here for site B2 (Fig. 6a) at 430 m, the previous estimate of lowland-derived (<500 m) FPOM at Óbidos can be almost doubled, to >60%. A similar estimate of >60% lowland CPOM ($\delta^{13}C = -28.8$‰), can be obtained using the $\delta^{13}C$ values for the highest altitude (-26.7‰) and Óbidos (-28.0‰) samples in Fig. 6a. The observation that most (~85%) of the mineral material transported by the Brazilian Amazon originates outside the lower basin (Gibbs 1967), whereas most (>60%) of the associated organic matter appears derived from drainage regions <500 m in altitude, suggests that much of the original particulate organic matter in these two size fractions is replaced during transport. This inference is especially pertinent to the FPOM fraction, which, although closely associated with mineral at relatively uniform loadings (Keil et al. 1997), appears to be largely exchangeable on the time scale of transport through the river/floodplain system. Detailed measurements of the comparative fluxes and compositions of the mineral and organic components of FPOM and CPOM through the upper river network will be necessary to definitively test this implication.

Whether the relatively consistent offsets in $\delta^{13}C$ and $\delta^{15}N$ between FPOM and UDOM components from the same water samples (Fig. 6b) are also a source effect is not presently clear. It might be that sources of organic matter at higher altitude are unusually depleted in ^{15}N, with the result that this signature fades downstream, along with the ^{13}C-enrichment of the corresponding organic carbon. This explanation is also consistent with evidence for a particularly strong inorganic nitrogen source in the upper drainage basin (Fig. 5), but the $\delta^{15}N$ of this fraction is presently unknown. Although riverine organic materials associated with suspended minerals are enriched versus dissolved counterparts in both ^{13}C and ^{15}N, as would be expected from a cumulative isotope effect, the relatively weak associations of large organic molecules with mineral surfaces should not directly cause appreciable stable isotope fractionation. It seems more likely that different molecule types exhibiting isotopically distinct isotopic compositions might be selectively partitioned between the mineral and water phase, leading (passively) to substantial isotope differences.

A comparison of lignin phenol yields (Λ) and stable carbon isotope compositions between the Beni system and the lower Madeira and mainstem (Fig. 7a) reveals more similarities than contrasts. The cropped scales used in Fig. 7 to highlight contrasts among riverine samples cover less than half of the total variability in each parameter exhibited by local plant sources (Hedges et al. 1994). Except for the previously discussed trend toward greater $\delta^{13}C$ values at extreme elevations, the stable carbon isotope compositions and lignin yields of the more downstream tributary samples (2–5) fall near the ranges measured over different stages of the

Table 6. Amino acid yields, in mg (100 mg OC)$^{-1}$, from individual riverwater size fractions.

Site	Fraction	ASP	GLU	HIS	SER	GLY	THR	ALA	TYR	MET	VAL	PHE	ILU	LEU	ARG	LYS	BALA	GABA	AABA	THAA
B1	CPOM	0.49	1.08	0.13	0.65	0.70	0.45	0.54	0.30	0.00	0.49	0.44	0.36	0.52	0.45	0.64	0.00	0.00	0.05	7.29
B1	FPOM	1.31	2.06	0.15	1.06	1.41	1.15	1.75	0.38	0.00	2.09	0.93	0.95	1.31	0.92	1.14	0.08	0.00	0.09	16.8
B1	UDOM	0.39	0.48	0.08	0.27	0.63	0.358	0.65	0.15	0.00	0.37	0.23	0.25	0.33	0.18	0.14	0.10	0.05	0.01	4.66
B2	CPOM	1.36	1.78	0.18	1.29	1.83	1.34	1.95	0.71	0.00	1.60	1.00	1.07	1.38	0.63	0.72	0.15	0.02	0.02	17.0
B2	FPOM	1.31	1.64	0.18	1.15	1.55	1.12	1.61	0.26	0.00	1.18	0.65	0.72	0.89	0.62	0.74	0.11	0.03	0.04	13.8
B2	UDOM	0.44	0.51	0.08	0.35	0.61	0.40	0.61	0.16	0.00	0.38	0.19	0.24	0.31	0.11	0.11	0.16	0.05	0.01	4.71
B3	CPOM	1.15	1.49	0.16	1.22	1.61	1.14	1.65	0.58	0.00	1.23	0.87	0.84	1.14	0.53	0.57	0.09	0.00	0.01	14.3
B3	FPOM	1.49	1.90	0.20	1.23	1.82	1.24	1.78	0.40	0.06	1.48	0.81	0.86	1.11	0.74	0.64	0.17	0.09	0.05	16.1
B3	UDOM	0.33	0.37	0.08	0.26	0.42	0.29	0.43	0.12	0.00	0.27	0.13	0.16	0.21	0.06	0.06	0.11	0.04	0.01	3.36
B4	CPOM	1.29	1.68	0.31	1.31	1.68	1.06	1.40	0.64	0.00	1.21	0.80	0.84	1.20	0.70	0.95	0.11	0.00	0.08	15.2
B4	FPOM	0.90	1.12	0.17	0.81	1.08	0.72	1.03	0.17	0.00	0.90	0.36	0.45	0.58	0.43	0.63	0.08	0.06	0.04	9.54
B4	UDOM	0.36	0.36	0.06	0.28	0.52	0.36	0.48	0.16	0.00	0.29	0.15	0.18	0.23	0.07	0.13	0.16	0.05	0.02	3.85
B5	CPOM	1.08	1.34	0.19	1.07	1.40	0.86	1.30	0.43	0.00	1.13	0.80	0.75	0.95	0.49	1.19	0.08	0.00	0.07	13.2
B5	FPOM	1.13	1.62	0.20	1.05	1.49	1.05	1.62	0.18	0.14	1.50	0.74	0.82	1.06	0.71	0.58	0.14	0.10	0.02	14.2
B5	UDOM	0.45	0.50	0.11	0.35	0.61	0.43	0.64	0.22	0.00	0.41	0.24	0.26	0.37	0.11	0.14	0.14	0.05	0.02	5.07
M	CPOM	1.38	1.61	0.42	1.41	2.06	1.15	2.01	0.74	0.00	1.57	0.91	1.06	1.43	0.72	0.85	0.10	0.00	0.00	17.4
M	FPOM	1.26	1.77	0.22	1.11	1.49	1.16	1.73	0.44	0.10	1.70	0.81	0.92	1.22	0.82	0.59	0.14	0.07	0.06	15.6
M	UDOM	0.45	0.49	0.11	0.35	0.76	0.44	0.68	0.23	0.00	0.40	0.25	0.26	0.35	0.12	0.21	0.17	0.06	0.03	5.36
R	CPOM	1.44	1.65	0.44	1.31	1.93	0.88	1.24	0.55	0.12	1.20	0.95	0.90	1.30	1.42	0.93	0.09	0.09	0.00	16.5
R	FPOM	2.31	2.27	0.50	1.37	2.56	1.49	1.97	1.10	0.62	1.60	1.19	1.07	1.78	1.72	0.28	0.23	0.21	0.00	22.2
R	UDOM	0.51	0.40	0.06	0.27	0.66	0.33	0.36	0.12	0.07	0.25	0.14	0.14	0.18	0.10	0.20	0.13	0.08	0.02	4.01
Z	CPOM	1.22	1.37	0.32	1.01	1.56	0.68	1.00	0.43	0.06	1.02	0.76	0.74	1.04	1.03	0.49	0.07	0.09	0.00	12.9
Z	FPOM	2.36	2.83	0.85	2.31	3.18	1.98	2.42	1.26	0.85	2.12	1.59	1.54	2.66	2.99	1.91	0.35	0.28	0.00	31.5
Z	UDOM	0.38	0.28	0.05	0.24	0.45	0.30	0.28	0.04	0.09	0.18	0.10	0.10	0.15	0.09	0.12	0.14	0.07	0.01	3.07

Rio Madeira and Amazon data are for one sampling April–May 1994 (Hedges et al. 1994). Abbreviations: ASP, aspartic acid; GLU, glutamic acid; HIS, histidine; SER, serine, GLY, glycine; THR, threonine; ALA, alanine; TYR, tyrosine; MET, methionine; VAL, valine; PHE, phenylalanine; ILU, isoleucine; LEU, leucine; ARG, arginine; LYS, lysine; BALA, β-alanine; GABA, γ-aminobutyric acid, AABA, α-aminobutyric acid, THAA, total hydrolyzable amino acid yield (all protein plus nonprotein amino acids, excluding ornithine). All other abbreviations are as in Tables 1 and 3.

hydrograph throughout the lower mainstem. Unfortunately, it was not possible to evaluate the lignin content of the small amount of coarse particulate matter recovered in the Achumani River. Nor can an average Λ range be given in Fig. 7a for UDOM samples from the mainstem, because few lignin data are available for such isolates other than those shown for Óbidos. Although coarse and fine particulates from the lower Beni appear slightly depleted in lignin versus mainstem averages, the offsets are small compared with the overall differences in average lignin phenol yields among woods (Λ = 19), tree leaves (Λ = 3.7), and submerged grasses (Λ = 9.1) from the lower basin (Hedges et al. 1986*a*). Except for the uppermost Achumani samples, all data plot near tree leaves, as is consistent with widespread (~50–80%) forests in the corresponding catchments (Table 1).

More pronounced compositional contrasts, however, are evident in comparisons of the weight ratios of total syringyl phenols to total vanillyl phenols (S : V) and total cinnamyl phenols to total vanillyl phenols (C : V) yielded by the various size fractions (Fig. 7b). From this plot, it is evident that coarse particles from the upper reaches of the Beni system are characterized by higher yields of syringyl and cinnamyl phenols. C : V values decrease with altitude, from an extreme of ~0.3 in the Alto Beni down to ~0.1 in the lower Beni and Rio Madeira, compared with a mean near 0.07 in the mainstem as a whole. This C : V trend is clearly evident, even though the extreme high-altitude CPOM sample from the Achumani was not analyzed. Given that even the C2 sample has a C : V greater than the range typical of tree leaves, an additional source of coarse plant material with a characteristically high cinnamyl phenol yield is indicated. On the basis of compositional patterns seen in the lower Amazon basin, the most likely additional lignin source is grass tissue, which has a C : V near 1 (Hedges et al. 1986*a*). Grasses are prevalent in the sparingly forested upper reaches (Sta. 1 and 2) of the Beni system (Table 2; Bird et al. 1992), although a predominant contribution from C4 species is not indicated by the stable carbon isotope data (Fig. 6b). The corresponding fine particulate samples from the upper Beni system also yield high relative concentrations of cinnamyl, but not syringyl, phenols (Fig. 7b). Pollen has been recognized recently as a potential source of particulate cinnamyl phenols in the 20–100-μm size range in some temperate climates (Keil et al. 1998; Hu et al. 1999) and may also contribute to the greater C : V ratios of the high-altitude CPOM and FPOM samples. Thus, the characteristically high C : V that was noted previously near the mouth of the Rio Madeira (Hedges et al. 1986*a*) is traceable (like ^{13}C enrichment) to high-altitude sources. In contrast, UDOM isolates from the same water samples do not exhibit a clear altitudinal trend in S : V or C : V, although as a group they exhibit lower S : V ratios than the other two fractions (Fig. 7b). This distinction may be in part linked to the unique degradation/partitioning history of the dissolved organic component.

Organic degradation—The Bolivian tributary samples provide an opportunity to determine whether the differences in extents of degradation among CPOM, FPOM, and UDOM

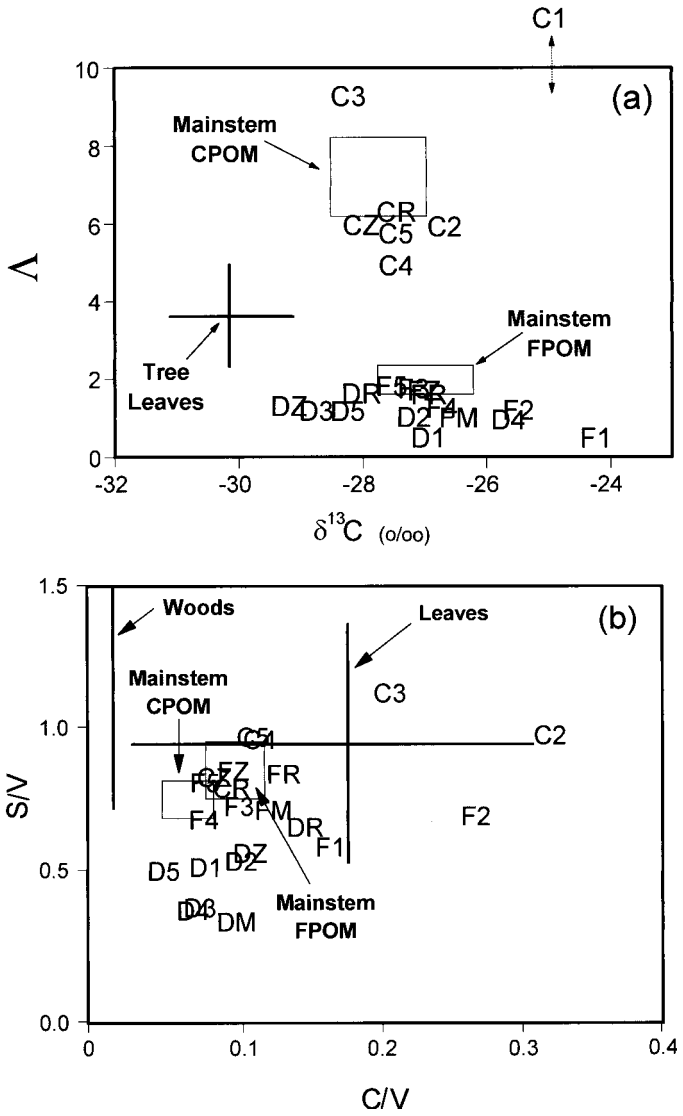

Fig. 7. Plots of: (a) total lignin phenol yields (Σ mg phenol/100 mg OC = Λ) versus $\delta^{13}C$ (per mil vs. PDB); and (b) total syringyl over total vanillyl (S : V) versus total cinnamyl over total vanillyl (C : V) phenols. In both frames, crosses indicate average compositions of different types of fresh vascular plant tissues from the lower Amazon basin (*see* Hedges et al. 1986*a* for full ranges of these plant compositions). The corresponding rectangles indicate the average compositions of coarse and fine particulate organic matter suspended throughout the lower Amazon mainstream (Fig. 1) at different stages of the hydrograph (n = 50, Hedges et al. 1986*a*). The two-ended arrow in (a) indicates the $\delta^{13}C$ value of the coarse particulate sample from the Achumani River, which was too small for lignin analysis (Λ is undefined). All symbols are as in Fig. 5.

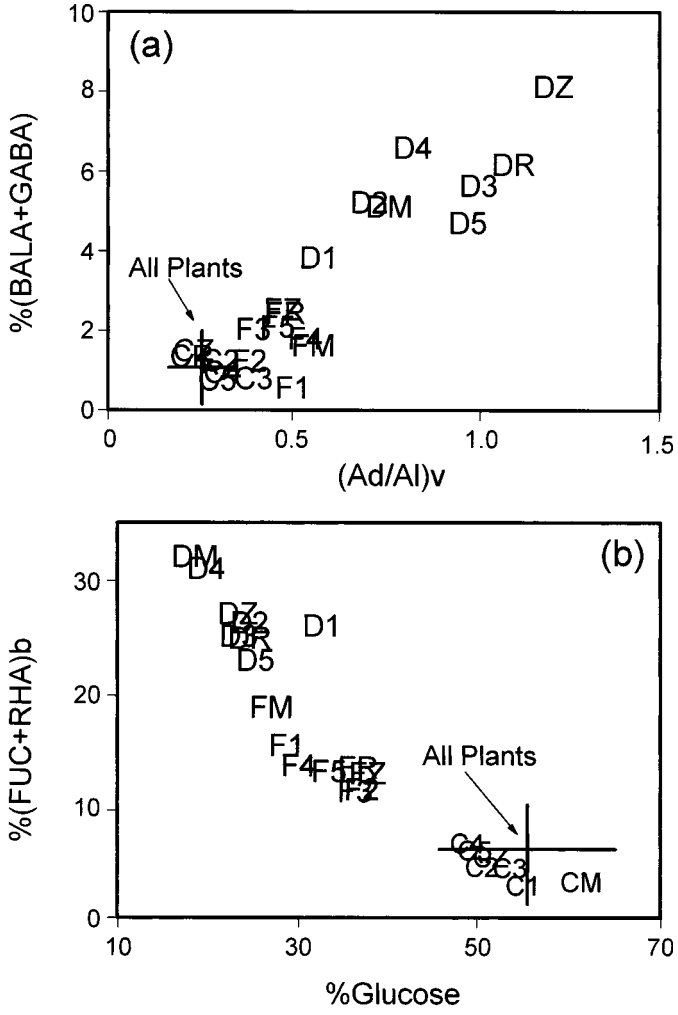

Fig. 8. Plots of: (a) the average mole percentages of β-alanine plus γ-aminobutyrioc acid, %(BALA + GABA), versus vanillic acid : vanillin ratio, (Ad : Al)v: as well as: (b) the weight percentage of fucose plus rhamnose, %(FUC + RHA), versus the overall weight percentage of glucose among all aldoses, (%Glucose). Crosses indicate the overall average compositions of four different types of fresh vascular plant tissues from the lower Amazon basin (Hedges et al. 1986*a*). All symbols are as in Fig. 5.

observed in the lower Amazon system (Hedges et al. 1994) also hold under the very different physical and hydrological conditions of the Andean headwaters. They also offer a means of testing the hypothesis, as suggested by the river continuum concept, that organic matter becomes progressively more degraded downstream in river systems (Vannote et al. 1980). Both assessments are strengthened because the general types of organic matter sources do not appear to vary greatly throughout the study reach (Fig. 7) and detailed compositional data are available for three different size fractions from each sampling site.

The first assessment of relative degradation is based on a comparison of the combined mole percentages of β-alanine plus γ-aminobutyric acid, %(BALA + GABA) versus the vanillic acid : vanillin ratio, (Ad : Al)v of the same samples. These two predominant nonprotein amino acids are known to become relatively more abundant with advanced microbial degradation (Lee and Cronin 1984; Cowie and Hedges 1994), whereas elevated vanillic acid yields are observed during fungal (Hedges et al. 1988) and bacterial (Opsahl and Benner 1995) degradation of lignin. In a cross plot of these variables (Fig. 8a), vascular plant tissues are conveniently located in a restricted lower region of %(BALA + GABA) = 0–1 and (Ad : Al)v = 0.15–0.35. As has been previously

noted for the lower basin, data for all the suspended CPOM samples from the upper Bolivian tributaries plot in the vicinity of undegraded plant material, indicating that the coarse organic fraction is relatively fresh. No correlation of degradation extent with altitude is evident among these plant debris. The corresponding fine particulate samples tend to clump at slightly higher values of %(BALA + GABA) = 1–3, with materials from the two highest altitudes (F1 and F2) plotting in a ''fresher'' region at the bottom of the nonprotein amino acid range. The (Ad : Al)v values of these two samples, (Ad : Al)v = 0.35–0.60, however, are located in the range of FPOM from the lower Beni system and mainstem. Data for the corresponding UDOM samples fall in a distinctly higher range of %(BALA + GABA) = 4–8 and (Ad : Al)v = 0.60–1.2 and exhibit a trend of more advanced degradation at increasing distance down the entire drainage network (Fig. 8a). Depetris and Kempe (1993) also have reported elevated mole percentages of nonprotein amino acids in dissolved versus suspended particulate material from the Paraná River, Argentina.

An independent carbohydrate-based perspective on organic matter degradation can be obtained from a plot (Fig. 8b) of the weight percentage of fucose plus rhamnose (on a glucose-free basis), %(FUC + RHA)b, versus the weight percentage of glucose, %Glucose, in hydrolysate mixtures from the same samples (Hedges et al. 1994). Because these two deoxy sugars typically increase during degradation, whereas glucose usually is selectively lost (Depetris and Kempe 1993), increased degradation of nonliving organic matter usually causes a trend toward the upper left of plots such as Fig. 8b. This graphical treatment again separates the three organic fractions into nonoverlapping regions that exhibit the same sequence of increased degradation (CPOM < FPOM < UDOM) evident in Fig. 8a for amino acids and lignin. Again, coarse particles plot in the range of fresh plant material. Also as before, downstream trends are not broadly evident for either of the two particulate fractions. The major contrast, versus Fig. 8a, is that the aldose compositions of the individual UDOM samples also do not vary systematically with order downstream. Thus, the processes that lead to greater degradation of lignin and amino acids in more downstream UDOM samples do not appear to similarly affect the coexisting carbohydrate component. That individual diagenetic parameters can respond with varying sensitivities to different types and stages of degradation is well known (e.g., Kempe and Depetris 1992; Cowie and Hedges 1994; Hedges et al. 1999), although the mechanisms involved are not yet clear.

These data demonstrate that the pattern of increasing degradation along the sequence CPOM < FPOM < UDOM holds for the Bolivian tributaries, as well as for lower Amazon system. Thus, the processes that imprint these compositional signatures must occur throughout the length of this immense drainage system. Such ubiquity is to be expected for biodegradation processes. These results also lend support to the size-reactivity continuum model of Amon and Benner (1996), in which larger organic substrates are viewed as being fresher and hence more rapidly cycled in aquatic systems. A complication for the Amazon system, however, is that the nominal size (e.g., as operationally defined by

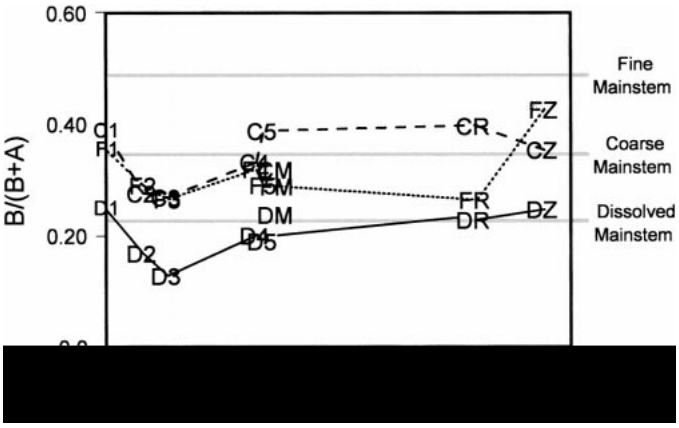

Fig. 9. A plot versus kilometer downstream of the combined mole percentage of two basic (B) amino acids (lysine plus arginine) divided by the combined mole percentage of two acidic (A) amino acids (glutamic plus aspartic acid) in coarse, fine, and dissolved organic matter from the study reach. The broad shaded lines indicate corresponding averages for the same three organic fractions from the lower Brazilian mainstem (Hedges et al. 1994). All symbols are as in Fig. 5.

filtration) of the FPOM fraction is determined by the dimensions of the mineral grains with which the much smaller organic molecules become associated. The same may be true for UDOM fractions from the higher tributaries, which contain predominantly inorganic matter (Fig. 5b). Although there is good reason to expect that organic molecules associated with mineral surfaces would be larger than those in the ambient solution (Hedges and Keil 1999), this relationship has not been demonstrated for the Amazon system. In addition, the percentage of DOM that can be removed by ultrafiltration increases down the Bolivian study reach (Fig. 4b), whereas the larger molecules making up these mixtures appear more degraded (Fig. 8a). This trend is inconsistent with the size-reactivity continuum model but is predicted by the river continuum concept. Neither model, however, takes into account that the reactivity, as well as the operational size, of organic substances can be greatly affected by association with minerals (Keil et al. 1994; Baldock and Skjemstad pers. comm.).

Partitioning histories—The Bolivian samples provide an opportunity to further test the hypothesis that preferential concentration of organic nitrogen, amino acids, and nitrogen-rich basic amino acids in fine particulate versus dissolved organic matter results from sequential sorption-based partitioning reactions within in the Amazon basin (Hedges et al. 1994; Devol and Hedges in press). This ''regional chromatography'' paradigm is based in part on laboratory evidence for selective sorption of nitrogen-rich organic molecules, exhibiting at least local cationic properties, onto the surfaces of mineral grains, which tend to be negatively charged within the pH range of most natural waters (e.g., Hedges 1978; Henrichs and Sugai 1993). Supporting, compositional, and dynamic field evidence from previous studies in the lower Amazon basin have also been presented (Hedges et al. 1986*b;* Keil et al. 1997). This partitioning model is partic-

ularly pertinent to tropical systems because it provides a possible means of physically retaining and protecting (Nelson et al. 1994) nitrogen in catchments that are microbially active and heavily leached. Preferential concentration of elemental nitrogen (Fig. 5) and total amino acids (Table 6) in FPOM versus UDOM has already been demonstrated for samples of the Beni system. This discussion will focus, therefore, on the distribution of acidic and basic amino acids among size fractions of the upper, versus lower, basin.

The relative distributions of basic (B) and acidic (A) amino acid types within the various size fractions of the Beni system are summarized in Fig. 9 as a plot of B : (A + B) versus kilometers downstream. Also shown in this figure are average B : (A + B) values for the same three size fractions from the lower Brazilian mainstream (Hedges et al. 1994). Both the coarse-particulate and dissolved organic fractions from the Beni system exhibit B : (A + B) ratios that closely resemble those seen in the lower mainstem. This similarity is to be expected for the CPOM fraction, which is composed of relatively fresh plant detritus that has not yet been subjected to sorptive partitioning and hence should contain an unaltered amino acid composition similar to the average (0.35) exhibited by living organisms (Cowie and Hedges 1992*b;* Keil et al. in press). The UDOM fraction is substantially depleted in basic amino acids versus plant tissues and CPOM from throughout Amazon system. The similarity of these higher altitude amino acid compositions to those from the lower basin supports parallel patterns of increased nitrogen and total amino acid in UDOM throughout the basin. Thus most lines of evidence agree in indicating that dissolved organic matter throughout the basin has been exposed to sorptive partitioning. Because none of the previous compositional patterns (that can be unambiguously traced to organic nitrogenous materials) vary appreciably with altitude or distance downstream (Tables 3, 5; Fig. 9), partitioning (like biodegradation) appears to affect dissolved organic molecules early in their transport history. This pattern therefore appears to be imprinted on the landscape of drainage basins as organic leachates percolate through soils or contact minerals in wetlands. The abundance of freshly weathered mineral particles at higher altitudes in the Andean hinterland may contribute to strong partitioning, even though steep slopes and high rainfall speed up water drainage rates.

Given the previous similarities, it is striking that fine particles suspended in the Beni system exhibit consistently low B : (A + B) ratios (~0.25–0.40) that never reach the mean (~0.5) typical of FPOM from the lower mainstem (Fig. 9). Both sample sets were analyzed by the same method, which is designed to minimize coulombic fractionation among amino acids (Cowie and Hedges 1992*a*). The upper reaches of the Beni system, however, are characterized by low ratios of DOC to both suspended fine particles and colloidal inorganic matter (Table 1; Fig. 3). Such high solids : water ratios favor increased partitioning, which leads to more pronounced fractionation of organic substances associated with the aqueous phase than with the coexisting inorganic matter. This notion is supported by the observation that, although the UDOM fraction of water samples from the Beni system are strongly depleted in basic amino acids (average = 4 mole%) versus both the FPOM (7%) and CPOM fractions (8%), their acidic amino acid fractions are almost identical (16–17 mole%). We do not know whether elevated solids : water ratios also prevail on the surrounding Andean upland, which is the ultimate source of most suspended inorganic particles in the Amazon River system (Gibbs 1967; Stallard 1988) and is a potential site of partitioning prior to the stream system.

It is also possible that the apparent difference in partitioning history is geologically related. Because particulate materials in the Beni system originate in part from physical erosion in a cold region of rapid uplift and sharp relief (Tables 1, 2), they should be less weathered chemically than particles stored for long time periods in the hot, acidic floodplains of the lower basin (Mertes 1990; Canfield 1997). Less extensive mineral weathering should lead to less mature partitioning of organic molecules in high-altitude rivers and hence to lower B : (A + B) ratios in the fine particulate fraction. This inference also is supported by field evidence for progressive weathering of coarse (Johnson and Meade 1990) and fine (Martinelli et al. 1993) minerals in lower floodplain deposits. On the other hand, suspended FPOM collected at Vargem Grande (Fig. 1) in the Amazon mainstem draining the Peruvian Andes exhibits a relatively high B : (A + B) ratio near 0.50, versus a value of about 0.25 for FPOM in the lower the Rio Madeira (Hedges et al. 1994). The observation that FPOM samples from two sites of such similar turbidity (~300–400 mg L^{-1}) and apparent Andean influence (Fig. 1) exhibit markedly different B : (A + B) ratios points toward causative factors in addition to physical setting, such as possible differences in bed rock mineralogy or weathering dynamics.

The previous distribution, diagenetic, and partitioning results for the Andean tributaries support many aspects of the regional chromatography model. For example, concentrations of FPOM throughout the Amazon system are controlled by TSS concentrations, as would be expected if the organic matter in this fraction is associated predominantly with minerals. CPOM occurs ubiquitously as relatively fresh plant debris, whose transport and fate is largely independent of sand-sized mineral matter. FPOM and UDOM are increasingly degraded to sufficiently small sizes to associate with silt- and clay-sized minerals and colloidal inorganic matter. The generally observed higher concentrations of elemental nitrogen, amino acids, and basic amino acids in FPOM versus UDOM indicate that selective association has occurred, with the notable exception of FPOM from the Beni/Madeira study reach.

The regional chromatography paradigm, however, does not explain all observations over the study reach, and a number of critical questions remain. For example, the sharply contrasting elemental, stable isotopic, and biochemical compositions of the UDOM and FPOM fractions suggest that the major components of these two dominant organic reservoirs are not in rapid, continuous exchange within the studied river system. The consistently lower extent of degradation of FPOM versus UDOM and depleted radiocarbon content of the FPOM fraction in the Brazilian Amazon (Hedges et al. 1986*b*) are particularly indicative of limited exchange. Most of the partitioning inferred from a constant loading or organic matter per unit surface area of fine minerals suspended in the lower river (Keil et al. 1997) and elevated concentra-

tion of nitrogenous organic matter in FPOM versus UDOM therefore must occur before introduction to the river. Soils have been proposed as the most likely site for this partitioning on the basis of their wide distribution, high mineral : DOM ratios, and the similarity between the elemental and lignin compositions of Amazon FPOM and ''typical soils'' (Hedges et al. 1994). We have not as yet, however, directly analyzed soils of the Amazon basin, and a previous study in the lower basin indicates that the river corridor may be a more important source of DOM than upland soils (McClain et al. 1997). Moreover, nitrogen-rich microbial remains are well known to concentrate with fine-grain mineral (Hedges and Oades 1997) and provide an alternate mechanism to partitioning for explaining the N richness of FPOM. Characterizations of local soils by the methods reported here, along with laboratory-controlled partitioning experiments that use locally pertinent mineral and DOM fractions, will be necessary to further test the validity of the regional chromatography model to the Amazon Basin.

Overview

The predictions of the river continuum concept can be similarly evaluated. Our observations do support the fundamental prediction that DOM degradation should become more extensive at more downstream sites (Fig. 8a). This trend, however, is not seen for either of the substantially fresher particulate fractions, which might be expected to cycle more rapidly. Also consistent with the predictions of Vannote et al. (1980) is the downstream increase in the percentage of DOM that can be recovered as UDOM (Fig. 4b) and hence is of greater nominal size. These authors' original rationale was that this trend would result as unreactive high molecular weight humic materials accumulate. This notion is counter to the size reactivity continuum model (Amon and Benner 1996), and the validity of size as a reactivity indicator becomes less straightforward when much of the organic matter in transit may be associated with mineral particles (previous discussion). A trend that is opposite of the river continuum model is that the CPOM : FPOM ratio increases downstream, from values near 0.01 at the uppermost station in the Andes to ratios on the order of 0.15 in the lower Madeira and Amazon (Table 3). This ratio may respond in the Amazon system more to particle transport dynamics than particle processing by in-stream biota (Richey et al. 1990).

Overall, the most robust contrast seen throughout the now expanded study reach continues to be compositional differences among CPOM, FPOM, and UDOM from the same waters, whether these fractions come from a first-order tributary in the high Andes or 3,000 km downstream in the Amazon mainstream. These patterns are not fully explained by either the river continuum or size reactivity continuum models, neither of which encompasses interactions of organic molecules with mineral phases. The regional chromatography paradigm does take into account organic/mineral association reactions that appear to strongly affect both fine particulate and dissolved organic materials, which together account for >90% of the TOC in transport. The regional chromatography model, however, is vague as to when and where organic interactions with minerals occur in drainage basins and how reversible and microbially mediated such processes might be. It is clear, however, from the relatively uniform compositions or organic materials (within size classes) throughout this immense drainage network that the processes responsible must occur predominantly outside the river channel, where vascular plant sources of these materials grow and degrade (*see* McClain et al. 1997). We appear to be at a stage of research for the Amazon system at which conceptual models require more testing by field studies and laboratory simulations that focus on degradation and partitioning processes occuring in soils and riparian zones.

References

AMON, R. M. W., AND R. BENNER. 1996. Bacterial utilization of different size classes of dissolved organic matter. Limnol. Oceanogr. **41:** 41–51.

BENNER, R. 1991. Ultra-filtration for the concentration of bacteria, viruses, and dissolved organic matter, p. 181–185. *In* D. C. Hurd and D. W. Spencer [eds.]. Marine particles: Analysis and characterization. American Geophysics Union.

———, AND J. I. HEDGES. 1993. A test of the accuracy of freshwater DOC measurements by high-temperature catalytic oxidation and UV-promoted persulfate oxidation. Mar. Chem. **41:** 161–165.

———, AND M. STROM. 1993. A critical evaluation of the analytical blank associated with DOC measurement by high-temperature catalytic oxidation. Mar. Chem. **41:** 153–160.

BIRD, M. I., W. S. FYFE, D. PINHEIRO-DICK, AND A. R. CHIVAS. 1992. Carbon isotope indicators of catchment vegetation in the Brazilian Amazon. Global Biogeochem. Cycles **6:** 293–306.

———, S. G. HABERLE, AND A. R. CHIVAS. 1994. Effect of altitude on the carbon-isotope composition of forest and grassland soils from Papua New Guinea. Global Biogeochem. Cycles **8:** 13–22.

CAI, D.-L., F. C. TAN, AND J. M. EDMOND. 1988. Sources and transport of particulate organic carbon in the Amazon River and Estuary. Estuar. Coast. Shelf Sci. **26:** 1–14.

CANFIELD, D. E. 1997. The geochemistry of river particulates from the continental USA: Major elements. Geochim. Cosmochim. Acta **61:** 3349–3365.

COWIE, G. L., AND J. I. HEDGES. 1992*a*. Improved amino acid quantification in environmental samples: Charge-matched recovery standards and reduced analysis time. Mar. Chem. **37:** 223–238.

———, AND ———. 1992*b*. Sources and reactivities of amino acids in a coastal marine environment. Limnol. Oceanogr. **37:** 703–724.

———, AND ———. 1994. Biochemical indicators of diagenetic alteration in natural organic matter mixtures. Nature **369:** 304–307.

DANKO, D. M. 1992. The digital chart of the world. GeoInfo Systems **2:** 29–36.

DEGENS, E. T., S. KEMPE, AND J. E. RICHEY. 1991. Biogeochemistry of major world rivers. Wiley.

DEPETRIS, P. J., AND S. KEMPE. 1993. Carbon dynamics and sources in the Paraná River. Limnol. Oceanogr. **38:** 382–395.

DEVOL, A. H., AND J. I. HEDGES. In press. The biogeochemistry of the Amazon River mainstem. *In* M. E. McClain and J. E. Richey [eds.], The biogeochemistry of the Amazon Basin and its role in a changing world. Oxford University Press.

EMBRAPA. 1981. Mapa de solos do Brasil, Escala 1 : 5,000,000.

Servico Nacional de Levantamento e Conservacao de Solos, Brasil.

ERTEL, J. R., J. I. HEDGES, A. H. DEVOL, J. E. RICHEY, AND N. RIBEIRO. 1986. Dissolved humic substances of the Amazon River system. Limnol. Oceanogr. **31:** 739–754.

ESRI. 1997. ARC/INFO version 7.1.1. Redlands, California.

GESCH, D. B., K. L. VERDIN, AND S. K. GREENLEE. 1999. New land surface digital elevation model covers the Earth. EOS **80:** 70–71.

GIBBS, R. J. 1967. Amazon River: Environmental factors that control its dissolved and suspended load. Science **156:** 1734–1737.

GUYOT, J. L., J. BOURGES, R. HOORELBECKE, M. A. ROCHE, H. CALLE, J. CORTES, AND M. C. BARRAGAN GUZMAN. 1988. Exportation de matières en suspension des Andes vers l'Amazonie par le Roi Beni, Bolivie. IAHS Publ. **174:** 443–451.

———, J. QUINTANILLA, M. CALLIDONDE, AND H. CALLE. 1992. Distribución regional de la hidroquímica en la cuenca Amazónica de Bolivia, p. 135–144. *In* Seminario sobre el PHICAB. La Paz, SENAMHI/IHH/ORSTOM/CANAPHI.

———, AND J. G. WASSON. 1994. Regional pattern of riverine dissolved organic carbon in the Amazon drainage basin of Bolivia. Limnol. Oceanogr. **39:** 452–458.

HEDGES, J. I. 1978. The formation and clay mineral reactions of melanoidins. Geochim. Cosmochim. Acta **42:** 69–76.

———, R. A. BLANCHETTE, K. WELIKY, AND A. H. DEVOL. 1988. Effects of fungal degradation on the CuO oxidation products of lignin: A controlled laboratory study. Geochim. Cosmochim. Acta **52:** 2717–2726.

———, W. A. CLARK, P. D. QUAY, J. E. RICHEY, A. H. DEVOL, AND U. DE M. SANTOS. 1986*a*. Compositions and fluxes of particulate organic material in the Amazon River. Limnol. Oceanogr. **31:** 717–738.

———, G. L. COWIE, J. E. RICHEY, AND P. D. QUAY. 1994. Origins and processing of organic matter in the Amazon River as indicated by carbohydrates and amino acids. Limnol. Oceanogr. **39:** 743–761.

———, AND OTHERS. 1986*b*. Organic carbon-14 in the Amazon River system. Science **231:** 1129–1131.

———, F. S. HU, A. H. DEVOL, H. E. HARTNETT, E. TSAMAKIS, AND R. G. KEIL. 1999. Sedimentary organic matter preservation: A test for selective oxic degradation. Am. J. Sci. **299:** 529–555.

———, AND R. G. KEIL. 1999. Organic perspectives on estuarine processes: Sorption reactions and consequences. Mar. Chem. **65:** 55–65.

———, AND J. M. OADES. 1997. Comparative organic geochemistries of soils and marine sediments. Org. Geochem. **27:** 319–361.

———, AND J. H. STERN. 1984. Carbon and nitrogen determinations of carbonate containing solids. Limnol. Oceanogr. **29:** 657–663.

HENRICHS, S. M., AND S. F. SUGAI. 1993. Adsorption of amino acids and glucose by Resurrection Bay (Alaska) sediment: Functional group effects. Geochim. Cosmochim. Acta **57:** 823–835.

HOLDRIDGE, L. R. 1947. Determination of world plant formations from simple climatic data. Science **105:** 367–368.

HU, F. S., J. I. HEDGES, E. S. GORDON, AND L. B. BRUBAKER. 1999. Lignin biomarkers and pollen in postglacial sediments of an Alaskan lake. Geochim. Cosmochim. Acta **63:** 1421–1430.

ITTEKKOT, V., AND R. ARAIN. 1986. Nature of particulate organic matter in the river Indus, Pakistan. Geochim. Cosmochim. Acta **50:** 1643–1653.

JOHNSON, M. F., AND MEADE, R. H. 1990. Chemical weathering of fluvial sediments during alluvial storage: The Macupanin Island point bar, Solimões River, Brazil. J. Sediment. Petrol. **60:** 827–842.

KEIL, R. G., L. E. MAYER, P. D. QUAY, J. E. RICHEY, AND J. I. HEDGES. 1997. Loss of organic matter from riverine particles in deltas. Geochim. Cosmochim. Acta **61:** 1507–1511.

———, D. B. MONTLUÇON, F. G. PRAHL, AND J. I. HEDGES. 1994 Sorptive preservation of labile organic matter in marine sediments. Nature **370:** 549–552.

———, E. C. TSAMAKIS, J. C. GIDDINGS, AND J. I. HEDGES. 1998. Biochemical distributions (amino acids, neutral sugars, and lignin phenols) among size-classes of modern marine sediments from the Washington coast. Geochim. Cosmochim. Acta. **62:** 1347–1364.

———, ———, AND J. I. HEDGES. In press. Early diagenesis of particulate amino acids in marine systems. *In* G. A. Goodfriend, M. J. Collins, M. L. Fogel, S. A. Macko, and J. F. Wehmiller [eds.], Perspectives in amino acid and protein geochemistry. Oxford University Press.

KEMPE, S., AND P. J. DEPETRIS. 1992. Factors controlling the concentration of particulate carbohydrates and amino acids in the Paraná River. Hydrobiologia **242:** 175–183.

KÖRNER, CH., G. D. FARQUHAR, AND Z. ROKSANDIC. 1988. A global survey of carbon isotope discrimination in plants from high altitude. Oecologia (Berl.) **74:** 623–632.

LEE, C., AND C. CRONIN. 1984. Particulate amino acids in the sea: Effects of primary productivity and biological decomposition. J. Mar. Res. **42:** 1075–1097.

LEEMANS, R. 1992. Global Holdridge Life Zone classifications. Digital raster data on a 0.5-degree geographic (lat/long) 360 × 720 grid. *In* Global Ecosystem Database Version 1.0: Disc A. NOAA National Geophysical Data Center.

LEOPOLD, L. B. 1994. A view of the river. Harvard Univ. Press.

LUDWIG, W., J.-L. PROBST, AND S. KEMPE. 1996. Predicting the oceanic input of organic carbon by continental erosion. Global Biogeochem. Cycles **10:** 23–41.

MARTINELLI, L. A., R. L. VICTORIA, J. L. I. DEMATTE, J. E. RICHEY, AND A. H. DEVOL. 1993. Chemical and mineralogical composition of Amazon River floodplain sediments, Brazil. Appl. Geochem. **8:** 391–402.

MCCLAIN, M. R., J. E. RICHEY, J. A. BRANDES, AND T. P. PIMENTEL. 1997. Dissolved organic matter and terrestrial-lotic linkages in the central Amazon Basin of Brazil. Global Biogeochem. Cycles **11:** 295–311.

MERTES, L. A. K. 1990. Hydrology, hydraulics, sediment transport and geomorphology of the central Amazon floodplain. Ph.D. thesis, Univ. of Washington, Seattle.

MEYBECK, M. 1982. Carbon, nitrogen, and phosphorous transport by world rivers. Am. J. Sci. **282:** 401–450.

MINSHALL, G. W., K. W. CUMMINS, R. C. PETERSEN, C. E. CUSHING, D. A. BRUNS, J. R. SEDELL, AND R. L. VANNOTE. 1985. Developments in stream ecosystem theory. Can. J. Aquat. Sci. **42:** 1045–1055.

MORAES, J. L., AND OTHERS. 1995. Soil carbon stocks of the Brazilian Amazon Basin. Soil Sci. Soc. Am. J. **59:** 244–247.

NELSON, P. N., M.-C. DICTOR, AND G. SOULAS. 1994. Availability of organic carbon in soluble and particulate fractions from a soil profile. Soil Biol. Biochem. **26:** 1549–1555.

NORDIN, C. F., C. C. CRANSTON, AND A. MJIA. 1983. New technology for measuring water and suspended-sediment discharge of large rivers, p. 1145–1158. *In* River sedimentation. Proc. 2nd Int. Symp. Water Resour. Electr. Power Press.

OPSAHL, S., AND R. BENNER. 1995. Early diagenesis of vascular plant tissues: Lignin and cutin decomposition and biogeochemical implications. Geochim. Cosmochim. Acta **59:** 4889–4904.

———, AND ———. 1997. Distribution and cycling of terrigenous dissolved organic matter in the ocean. Nature **386:** 480–482.

POST, W. M., W. R. EMANUEL, P. J. ZINKE, AND A. G. STANGENBERGER. 1982. Soil carbon pools and world life zones. Nature **298:** 156–159.

———, J. PASTOR, P. J. ZINKE, AND A. G. STANGENBERGER. 1985. Global patterns of soil nitrogen storage. Nature **317:** 613–616.

QUAY, P. D., D. O. WILBUR, J. E. RICHEY, J. I. HEDGES, A. H. DEVOL, AND R. VICTORIA. 1992. Carbon cycling in the Amazon River: Implications for the ^{13}C compositions of particles and solutes. Limnol. Oceanogr. **37:** 857–871.

RADAMBRASIL. 1984. Levantamento de recursos naturais. Vol. 3–20, 22, 25, 26. Departamento Nacional da Producão Mineral.

RICHEY, J. E., J. I. HEDGES, A. H. DEVOL, P. D. QUAY, R. VICTORIA, L. MARTINELLI, AND B. R. FORSBERG. 1990. Biogeochemistry of carbon in the Amazon River. Limnol. Oceanogr. **35:** 352–371.

———, R. H. MEADE, E. SALATI, A. H. DEVOL, C. F. NORDIN, JR., AND U. DOS SANTOS. 1986. Water discharge and suspended sediment concentrations in the Amazon River: 1982–1984. Water Res. **22:** 756–764.

SEKULIN, A. E., A. BULLOCK, AND A. GUSTARD. 1992. Rapid calculation of catchment boundaries using an automated river network overlay technique. Water Resour. Res. **28:** 2101–2109.

SKOOG, A., AND R. BENNER. 1997. Aldoses in various size fractions of marine organic matter: Implications for carbon cycling. Limnol. Oceanogr. **42:** 1803–1813.

STALLARD, R. F. 1988. Weathering and erosion in the humid tropics, p. 225–246. *In* A. Lerman and M. Meybeck [eds.], Physical and chemical weathering in geochemical cycles. Kluwer.

STAUB, B., AND C. ROSENZWEIG. 1992. Global Zobler soil type, soil texture, surface slope, and other properties. Digital raster data on a 1-degree geographic (lat/long) 180 × 360 grid. *In* Global Ecosystem Database Version 1.0: Disc A. NOAA National Geophysical Data Center.

STONE, T. A., P. SCHLESINGER, R. A. HOUGHTON, AND G. M. WOODWELL. 1994. A map of the vegetation of South America based on satellite imagery. Photogrammetric Eng. Remote Sensing **60:** 541–551.

THENG, B. K. G. 1979. Formation and properties of clay–polymer complexes. Elsevier.

VANNOTE, R. L., G. W. MINSHALL, K. W. CUMMINS, J. R. SEDELL, AND C. E. CUSHING. 1980. The river continuum concept. Can. J. Fish. Aquat. Sci. **37:** 130–137.

Received: 4 November 1999
Accepted: 15 May 2000
Amended: 19 June 2000